Applications des détecteurs cryogéniques à la métrologie des rayonnements ionisants et analyse de matériaux

Matias Rodrigues

CEA / LNE-LNHB

1. Photon spectrometry

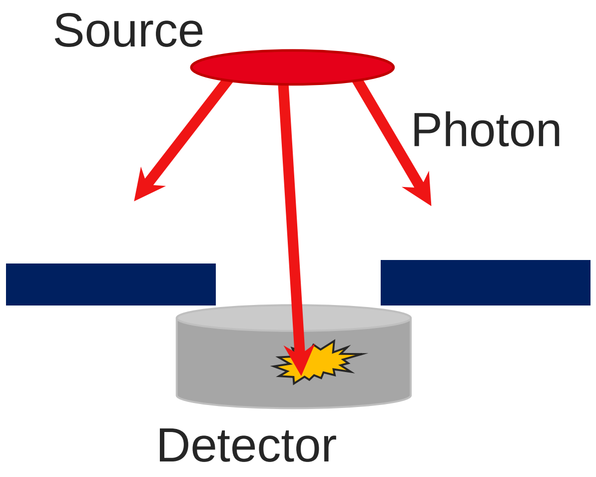

- **Detection efficiency = geometrical efficiency × intrinsic efficiency**
- **Source:**
  - Radionuclides
  - Material excited by a beam (charged particles (PIXE) or Synchrotron facilities (i.e. XRF), electrons)

2. Decay energy spectrometry

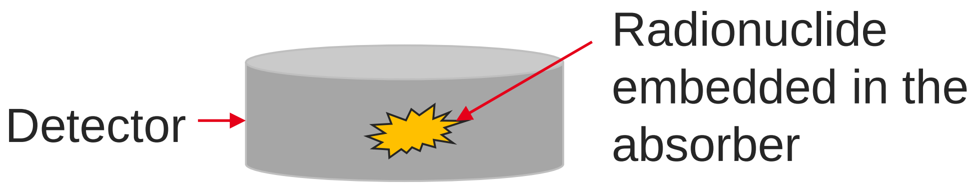

<u>4π geometry</u>

- **Detection efficiency ≈ intrinsic efficiencies ≈ 1 for charged particles**

- 1 pulse / decay = summed of many particle energies

Particles emitted per decay measured in coincidence

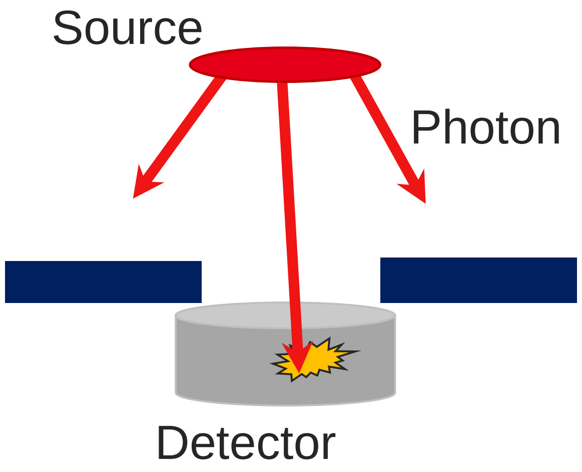

1. Photon spectrometry

Quantitative analysis by energy dispersive spectrometry

Source of radiations

- **Composition**
  - Activity
  - Elemental analysis
- **Fundamental parameters**
  - Emission probabilities
  - Characteristic energies
  - …

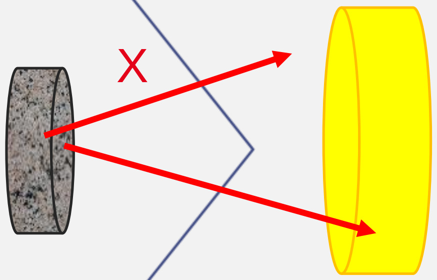

Detector

$\delta V \propto E$

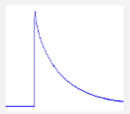

pulse

Electronics & DAQ

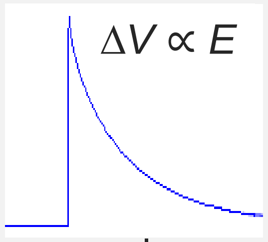

pulse

Pulse analysis

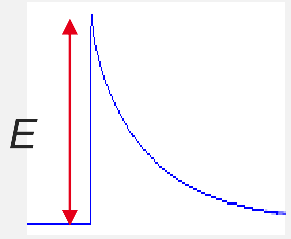

Spectrum processing

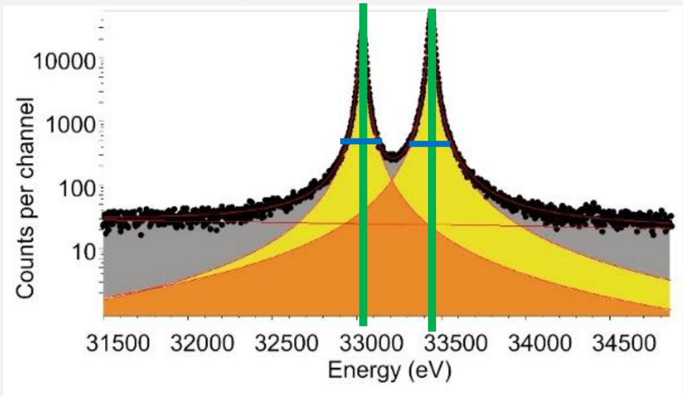

Measurand

- **Count / peak / time**
- **Energy**
- **Peak width**

Spectrum distorsions of the energy spectrum

Source of radiations

- Self absorption
- Inhomogeneity
- Auto-fluorescence

•Composition
•Fundamental parameters

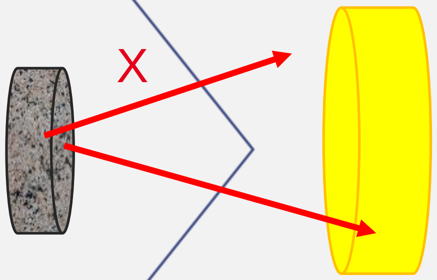

Detector

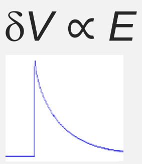

- **Detection efficiency**
- **Response function**
- **Energy non-linearity**

Electronics & DAQ

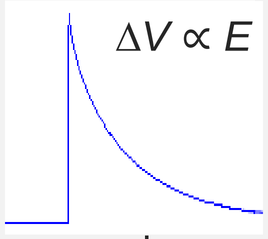

- Slew rate
- Non-linearities
- Gain drift

Pulse analysis

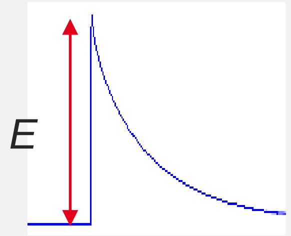

- Energy estimation
- Pile-ups and pulse rejection
- Live time

Spectrum processing

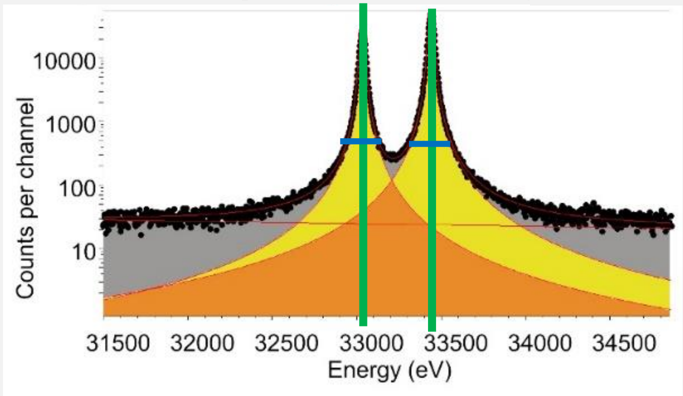

Measurand

- **Count / peak / time +/- σ**
- **Energy +/- σ**
- **Peak width +/- σ**

Spectrum distorsions lead to type B uncertainties or systematic errors

Measurand	Associated uncertainty	
	Type A	**Type B**

Count *N* / peak / time	• Counting statistics
	$\sigma_N = \sqrt{N}$
		• Efficiency calibration
		• Dead time measurement
		• **Spectrum processing**
		  • Inappropriate functions
		  • Overlapping peaks

Energy	• **Energy resolution**
	• Counting statistics
	$\sigma_E = \frac{FWHM}{2.35 \times \sqrt{N}}$
		• Energy calibration
		• **Spectrum processing**
		  • Inappropriate functions
		  • Overlapping peaks

Line width	• **Energy resolution**
	• Counting statistics
		• **Spectrum processing**
		  • Inappropriate functions
		  • Overlapping peaks

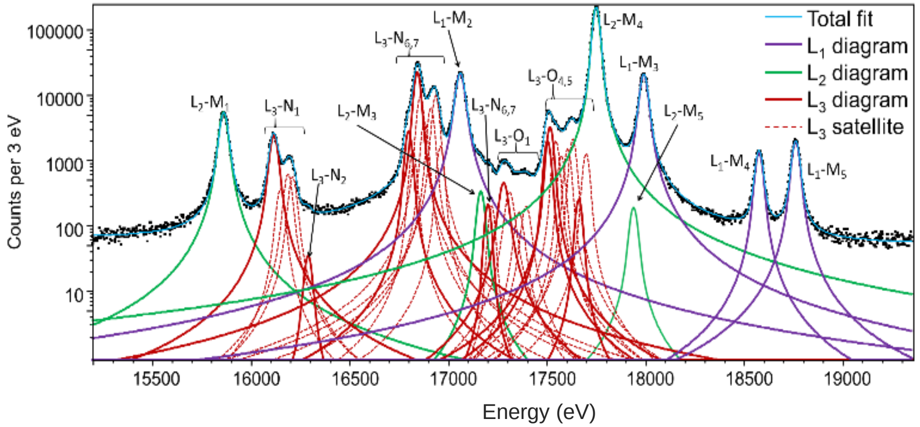

- Advantage of cryogenic detectors is their **very high resolving power**
- Advantage on the condition of a **Gaussian response function** at the peaks

Spectrum distortion due to bad thermal conductivity of the absorber

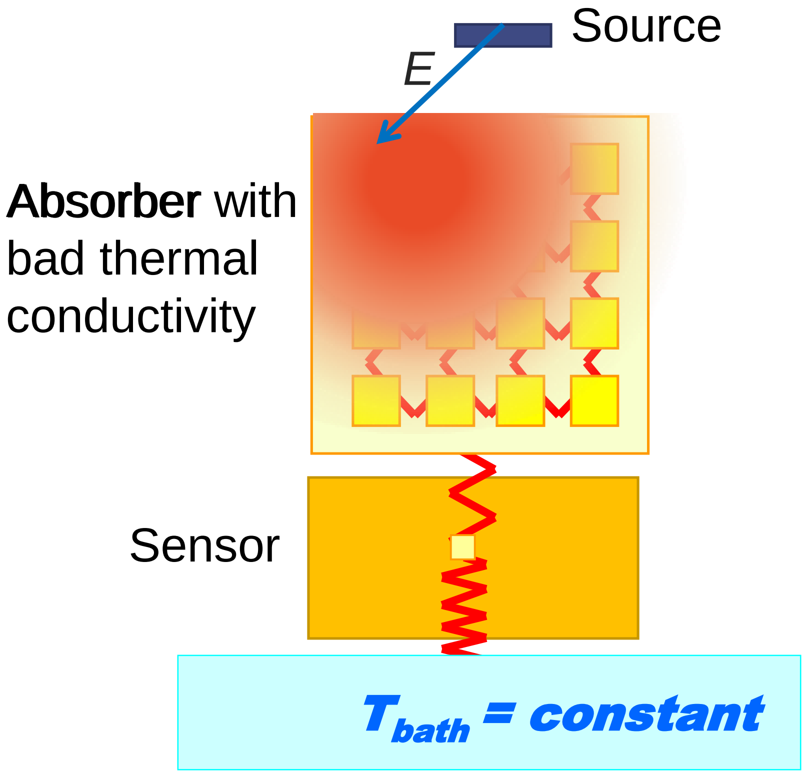

Pulse with slow rise time

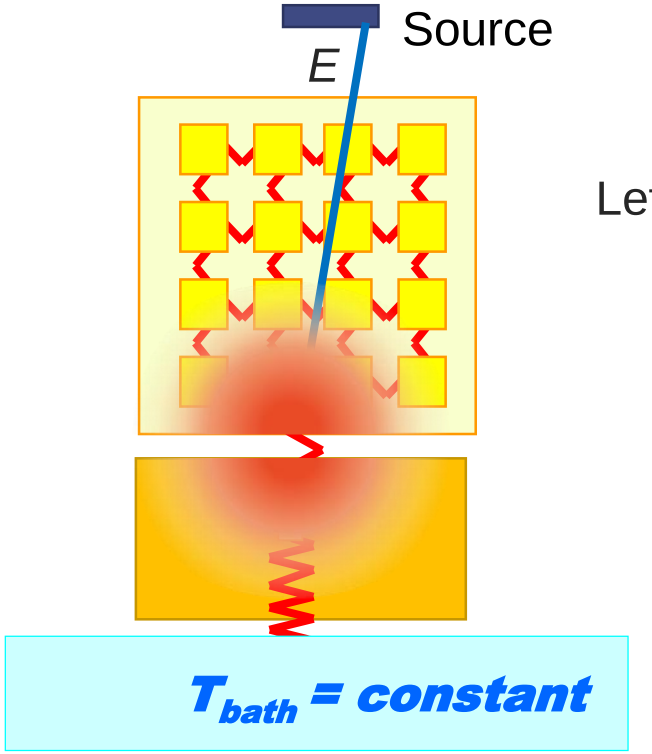

Pulse with faster rise time

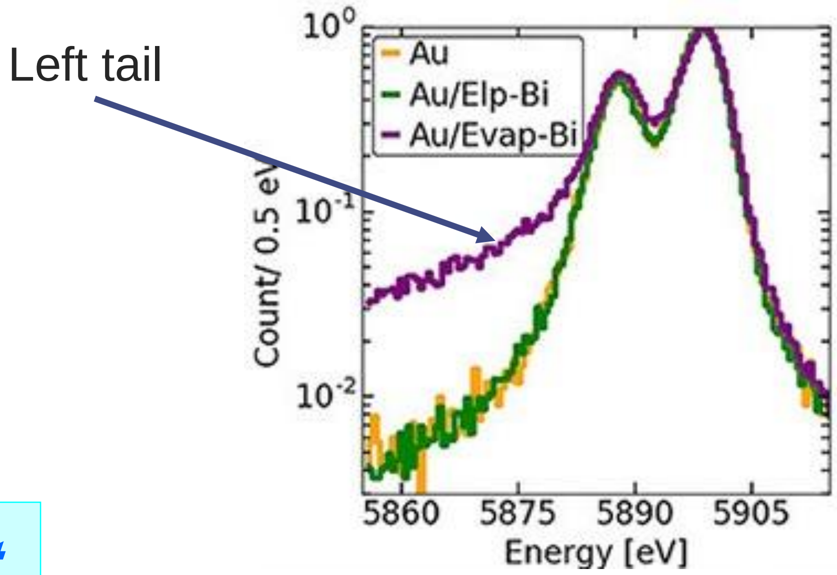

Divan, R. et al.. Appl. Phys. Lett. 111, 192602 (2017).

- Different pulse shapes as a function of the interaction position
  → Left tails or/and degraded energy resolution
- Au material is a good absorber choice for efficiency and thermalisatio
  →Price to pay is the higher specific capacity of Au

Spectrum distortions due to bath temperature fluctuations

The sensor is a very sensitive thermometer to the bath temperature → pulse height depends on the temperature
→ Pulse height drift with time

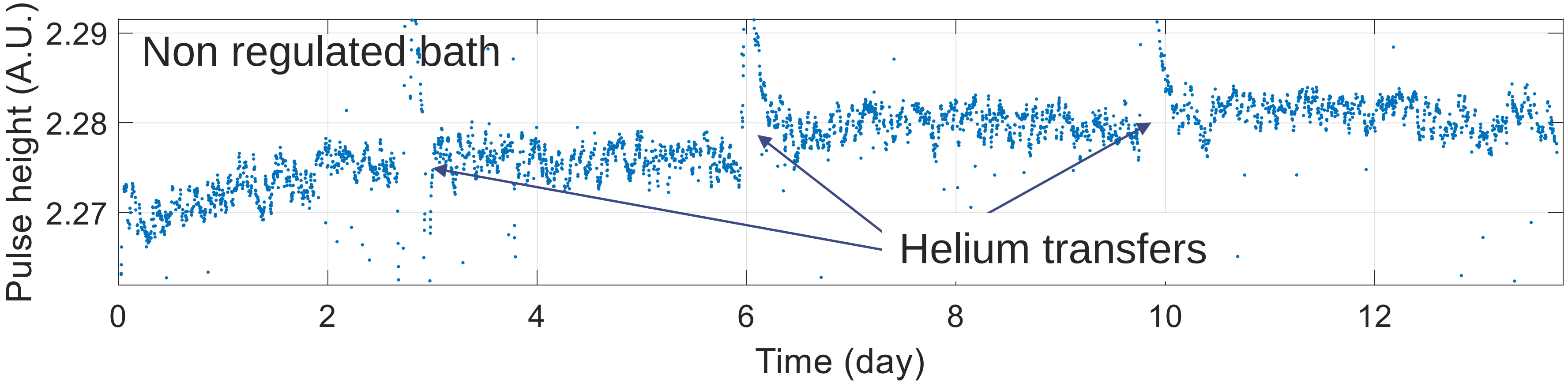

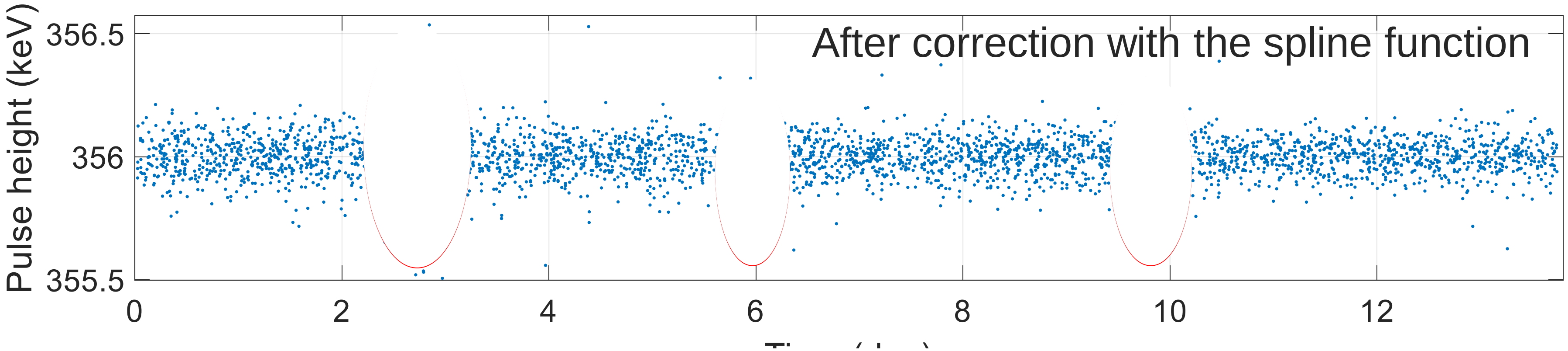

Three conditions for a good correction:

- a line in the spectrum with sufficient count rate
- a line with a relatively high resolving power
- the detector must be linear with the energy and temperature fluctuations

Spectrum distorsions from the pile-ups on the decay

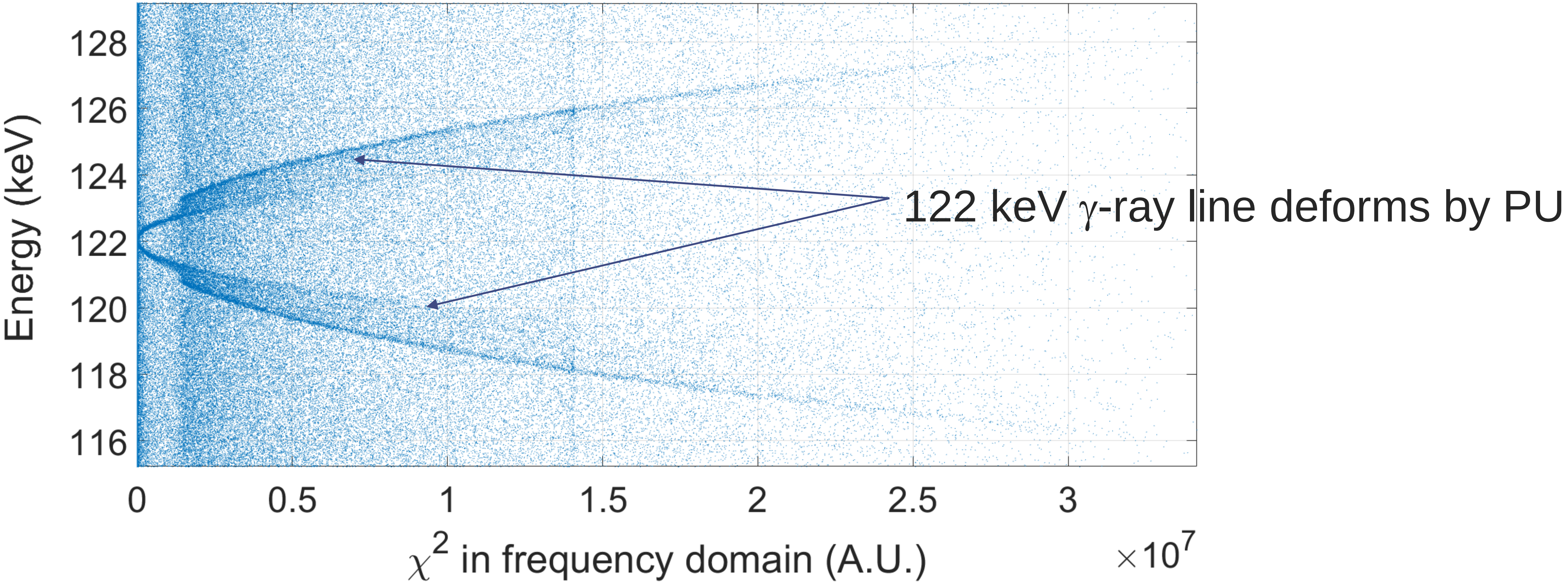

- χ^2 value depends on the pulse height
- It is a continuous distribution

→ Pile-up is a cause of peak distorsion

Spectrum distorsions for pixelated absorbers (1/2)

- <u>Spectrum co-adding</u>
  - The different pixels may have :
    - different non-linearities
      → The sum of Gaussian with different means is not a Gaussian
    - different energy resolutions
      →The sum of Gaussian with different widths is not a Gaussian

→ Co adding the individual spectra can lead to spectrum distortion

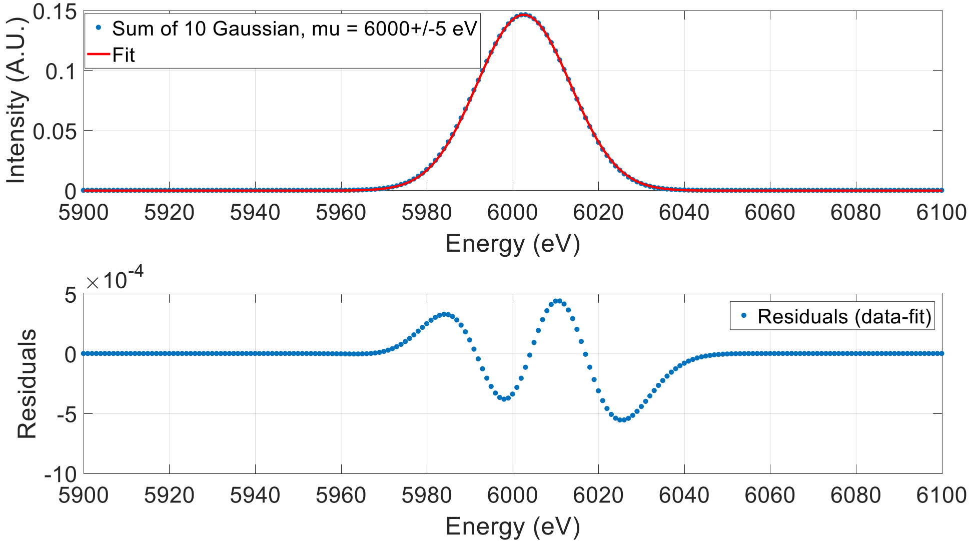

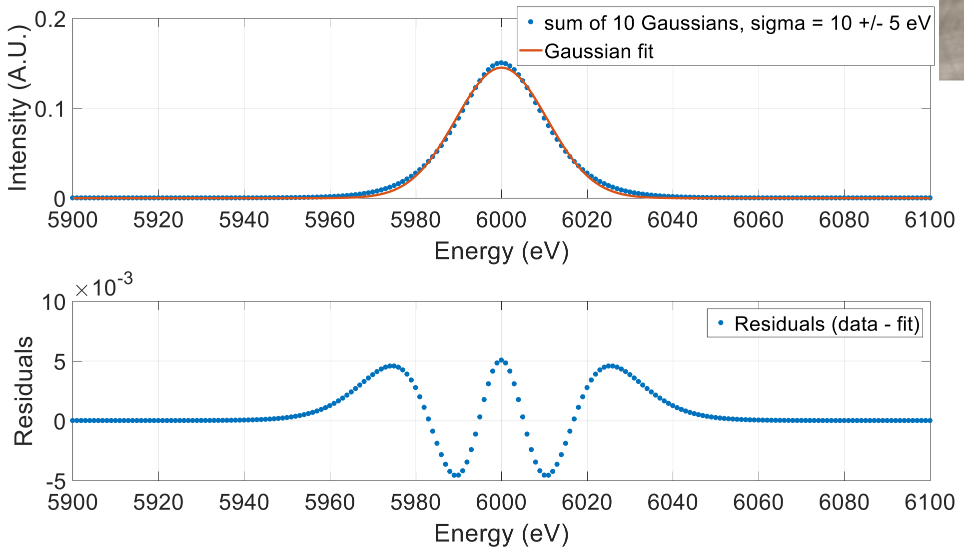

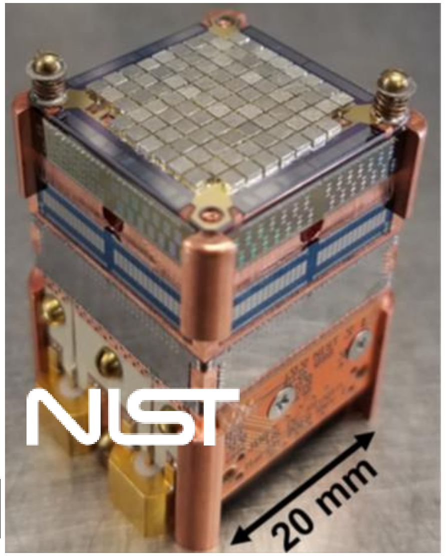

Spectrum distorsions for pixelated absorbers (2/2)

- Thermal cross talk
  - Between sensor / Si chips

Left tails probably caused by 60 keV in the Si chips

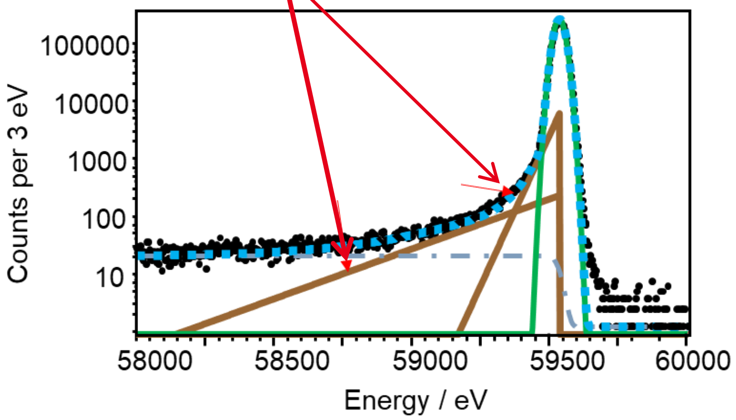

Matias Rodrigues *et al* 2023 *Metrologia* **60** 025005
DOI 10.1088/1681-7575/acb99f

  - Between sensors on a same chip

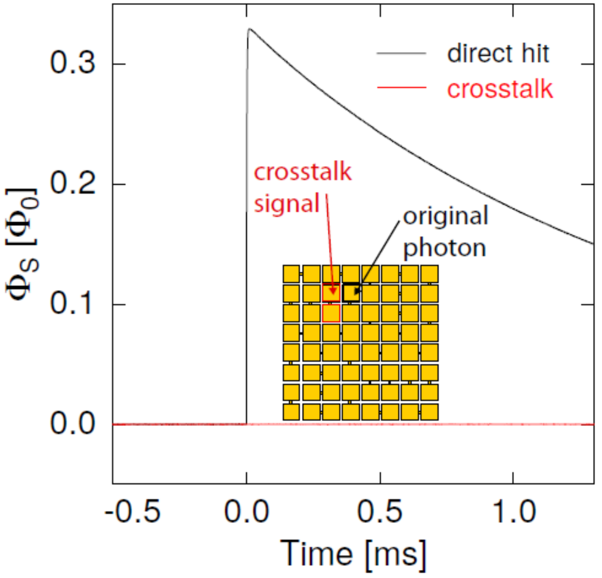

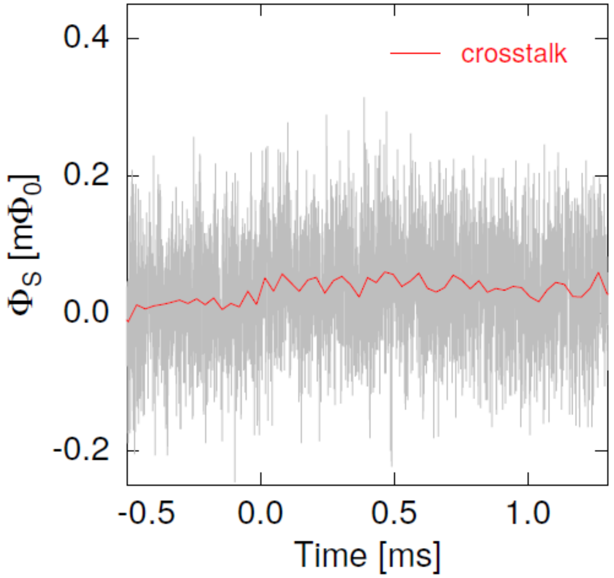

Development and characterization of two-dimensional metallic magnetic calorimeter arrays for the high-resolution X-ray spectroscopy. D. Hengstler. PhD Thesis. KIP Heidelberg
DOI: 10.11588/heidok.00023815

Applications using quantitative analysis with low temperature detectors

High energy resolution LTDs are useful for applications :

- with very complex spectra, i.e. where semiconductor detector resolution is useless
- where source having low emission rate, i.e. where the efficiency of WDS is too useless
- with relaxed data taking time (metrology)

Applications using cryogenic detectors	Count / peak	Energy	Natural line width	Ref.
Safeguards	X			[1]
Elemental & chemical analysis	X	X		[2]
Synchrotron applications	X	X		[3]
^{229m}Th for nuclear clock		X		[4]
QED and exotic atom studies		X		[5, 6]
Fundamental parameters	X	X	X	[7]
Decay data	X	X		[8,9]

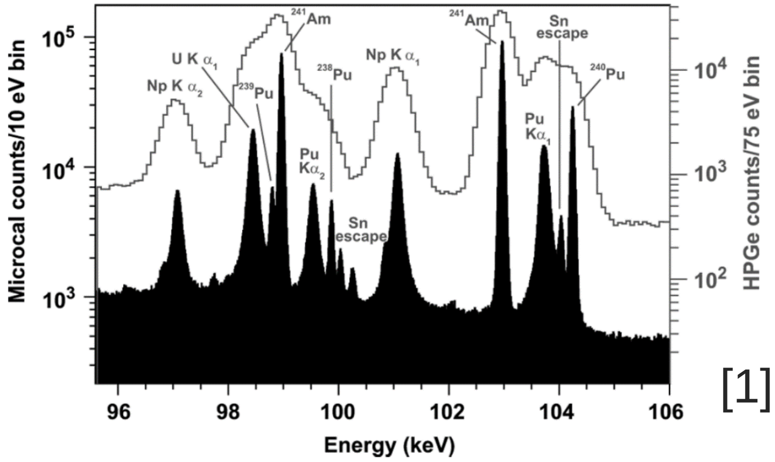

[1]

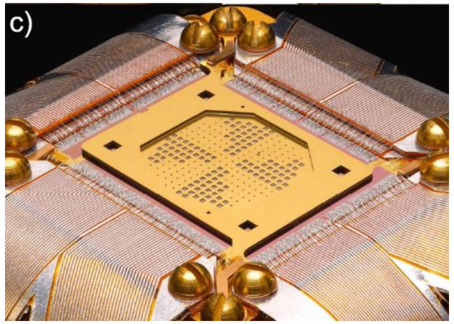

[3]

[1] Winkler R. et al. , *NIM A*, 770, 203 (2015).
[2] Carpenter, M.H., *J. Low. Temp. Phys.* 200, 437–444 (2020).
[3] Ullom J. N. et al. *Synchrotron Radiation News* 27, 24 (2014).
[4] Sikorsky T. et al. *Phys. Rev. Lett*. 125, (2020).
[5] Okumura T. et al. *Phys. Rev. Lett*. 130, 173001 (2023)
[6] Herdrich, M.O. *et al. Eur. Phys. J. D* **77**, 125 (2023)
[7] Fowler J. W. et al *Metrologia* 58 015016 (2021)
[8] Kim, G.B., *J. Low. Temp. Phys.* 199, 1055–1061 (2020)
[9] R. Mariam, Spec. Acta Part B: 187, 106331 (2022)

"Absolute" photon emission intensities (PEIs)

- Absolute PEIs: I = number of photons at E per 100 decays
- Essential decay parameter for quantitative analysis by photon spectrometry
- Absolute PEIs are challenging to measure accurately with standard deviation < 1%...

$$I(E) = \frac{N_{FEP}(E)}{A(t) \cdot \varepsilon_{FEP}(E) \cdot \Delta t}$$

N_{FEP}: counts in the Full Energy Peak (FEP)
ε_{FEP} : FEP detection efficiency
$A(t)$: source activity
Δt : live time

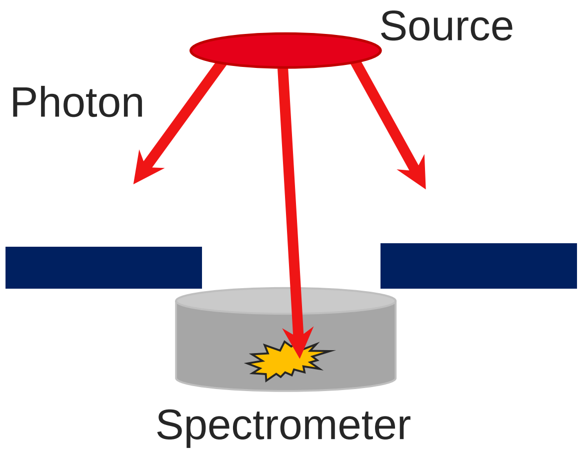

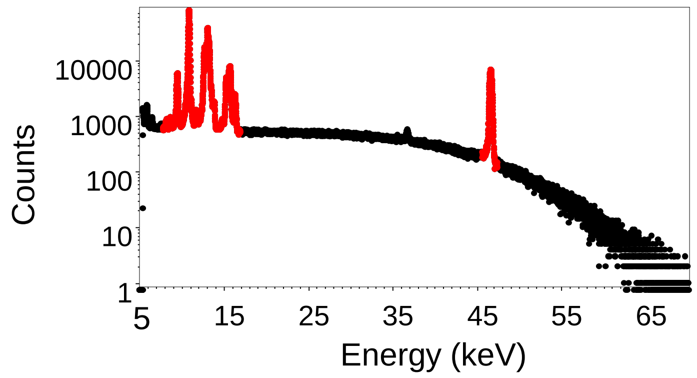

- $\varepsilon_{FEP}(E)$ is the product of $\varepsilon_{int.}(E) \times f_{geo}$ where $\varepsilon_{int.} = f(E) < 1$

f_{geo} : geometrical factor between source-collimator-absorber
$\varepsilon_{int.}$: intrinsic detection efficiency

- **ε_{FEP} and $\varepsilon_{int.}$ are difficult to calibrate accurately**

SMX3: A dedicated MMC for L X-ray spectrometry of actinides

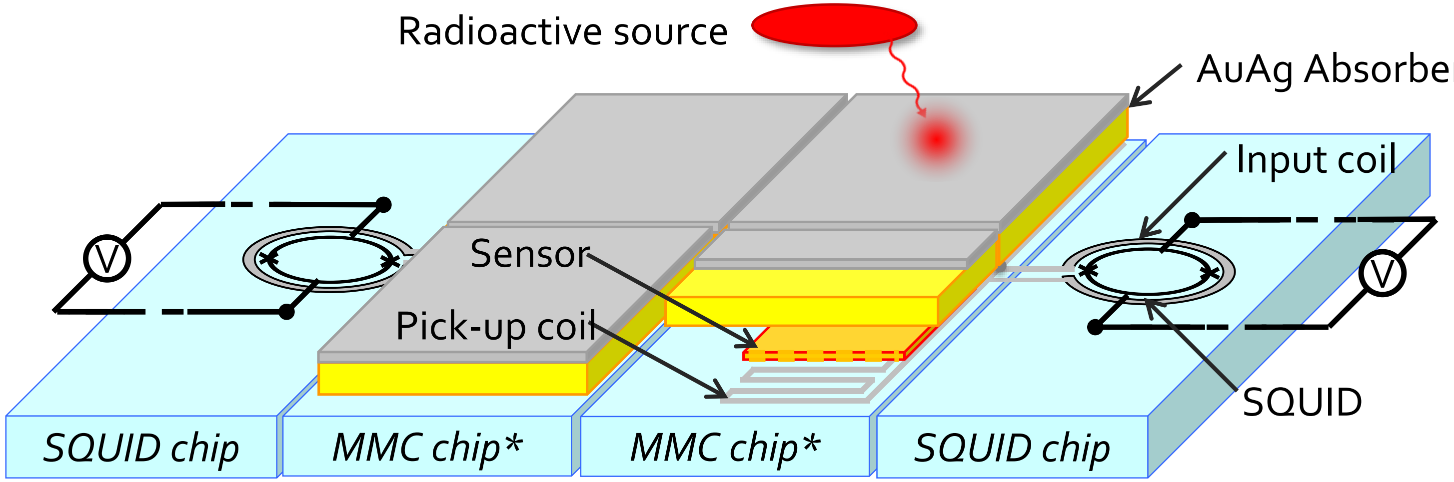

MMC chip optimized and produced by KIP Heidelberg

- Energy resolution FWHM of 22 - 40 eV
- Count rate of 10 – 20 s^{-1} ($\tau_d \approx 4$ ms)
  → Few 10^6 counts / week
- 4 absorbers of 1 mm^2, 50 μm of Au + 17 μm of Ag thick
  - Intrinsic efficiency > 99% for 10-25 keV
  → easier efficiency calibration

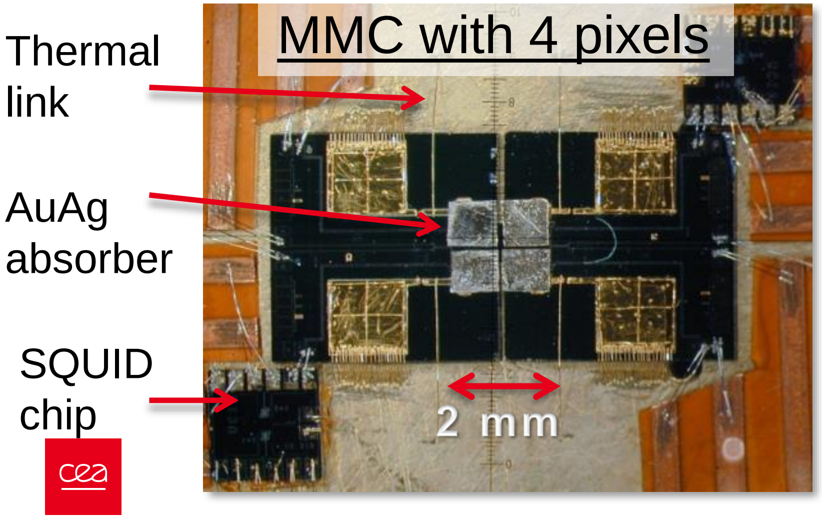

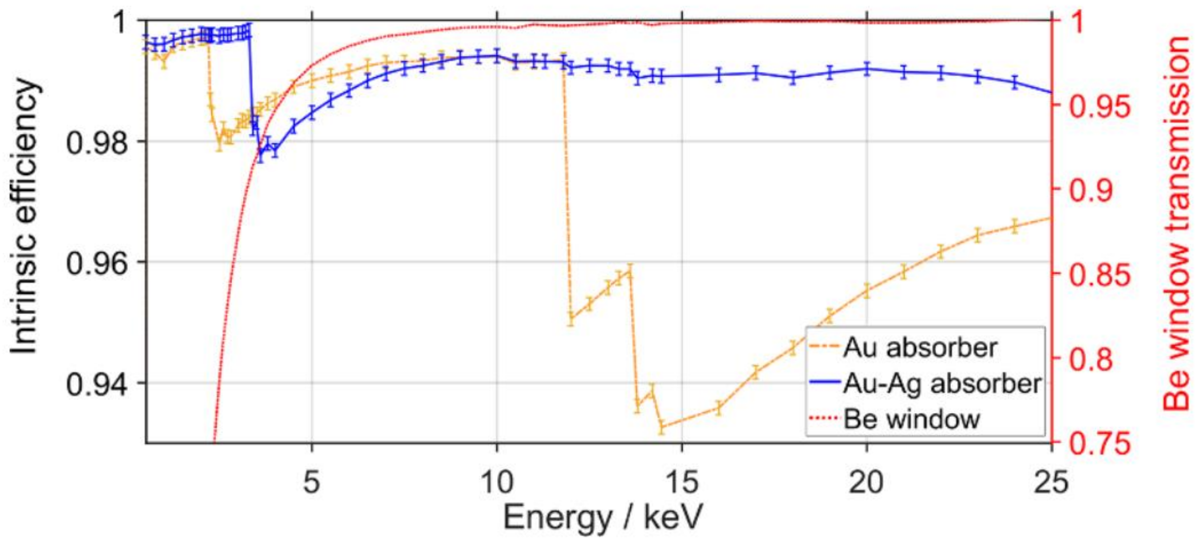

Response function of SMX3 at the full energy peaks (FEPs)

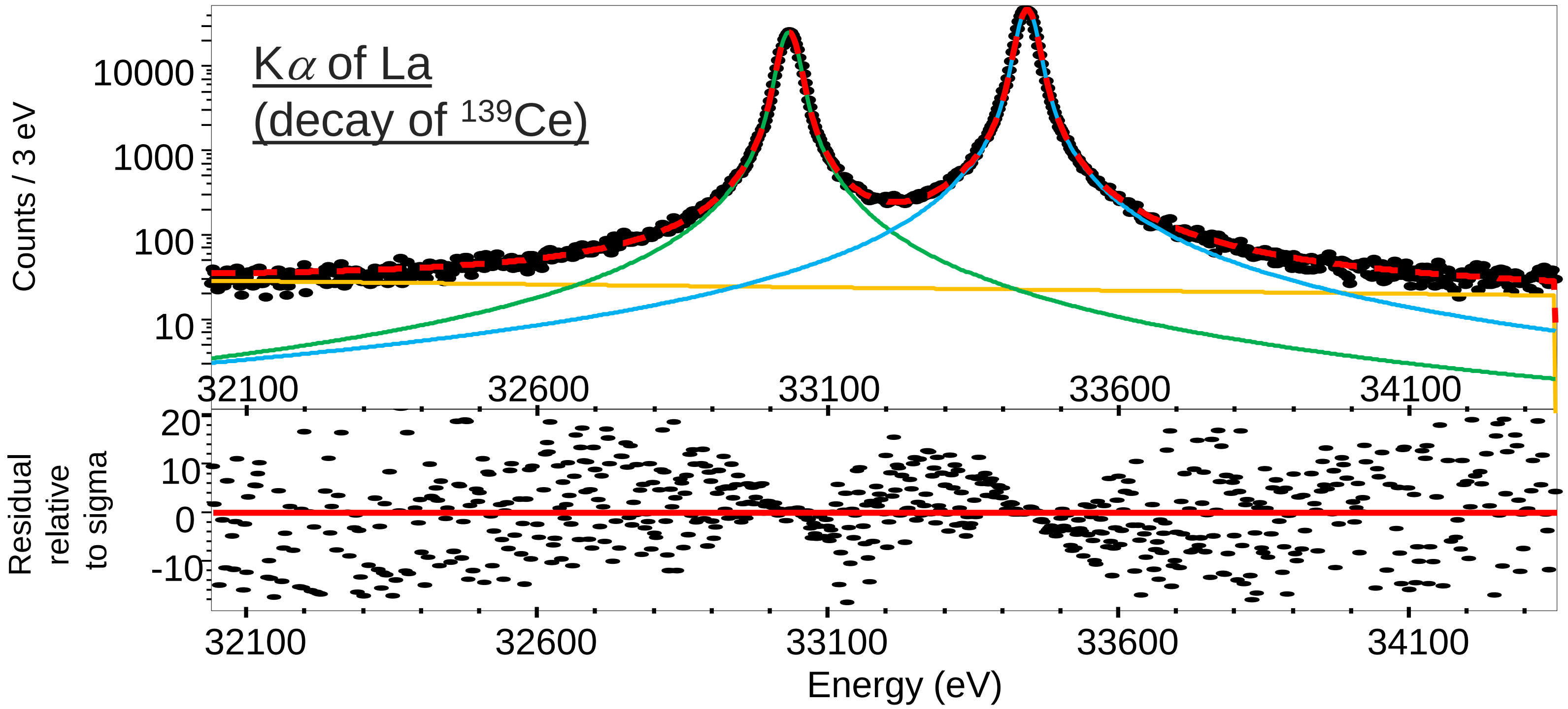

- 1x10⁶ counts in Kα
- Fit with free parameters

Line	Gaussian width	Lorentzian Width		
		This work	Krauss [1]	Campbell [2]
$K\alpha_1$	23.47 eV	18.44 eV	17.78 eV	17.55 eV
$K\alpha_2$	23.62 eV	17.78 eV	17.51 eV	17.32 eV

- No observed tail
- Good agreement between Lorentzian widths

→ Nearly Gaussian response at FEP

[1] Krauss M. O. Journal of Physical and Chemical Reference Data 8, 329–338 (1979)
[2] Campbell, J. L., & Papp, T. Atomic Data and Nuclear Data Tables Vol. 77, pp. 1–56 (2001)

Measurements of two ^{241}Am sources with different activities

1st measurement: α spectrum

- ^{241}Am source of 1.8 kBq
- Lower MMC sensitivity
- No Be window
- FWHM resolution of 3.3 keV

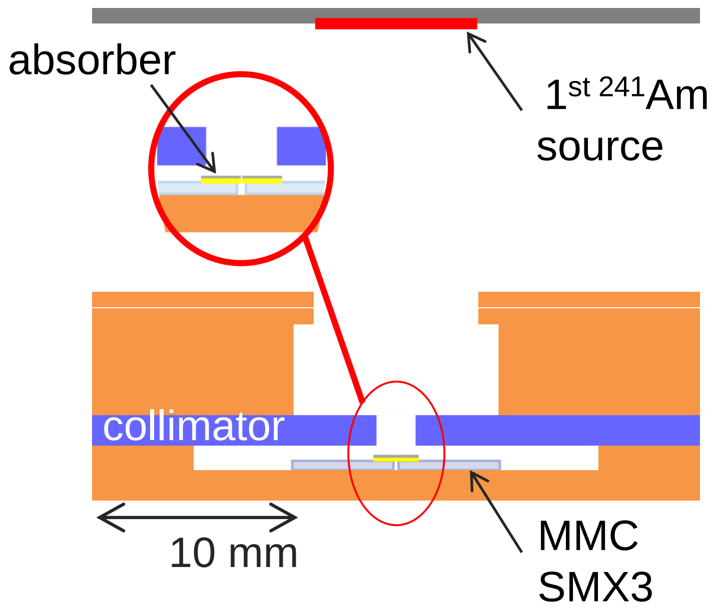

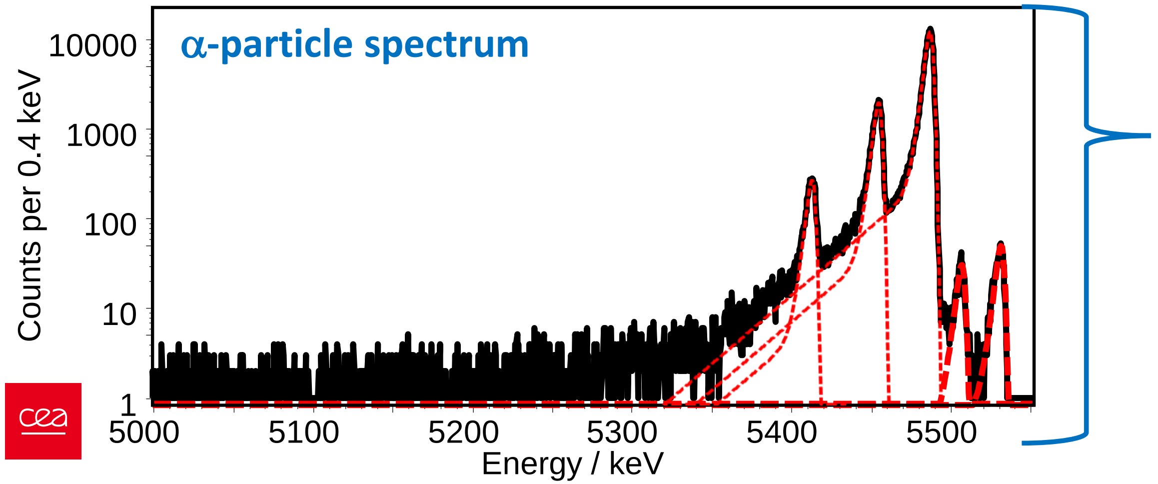

$\rightarrow n_\alpha$

Measurements of two ^{241}Am sources with different activities

1st measurement: α spectrum

- ^{241}Am source of 1.8 kBq
- Lower MMC sensitivity
- No Be window
- FWHM resolution of 3.3 keV

2nd measurement: X-ray spectrum

- ^{241}Am source of 32 kBq
- High MMC sensitivity
- Be window to stop the α-particles
- spectrum FWHM resolution of 28 eV

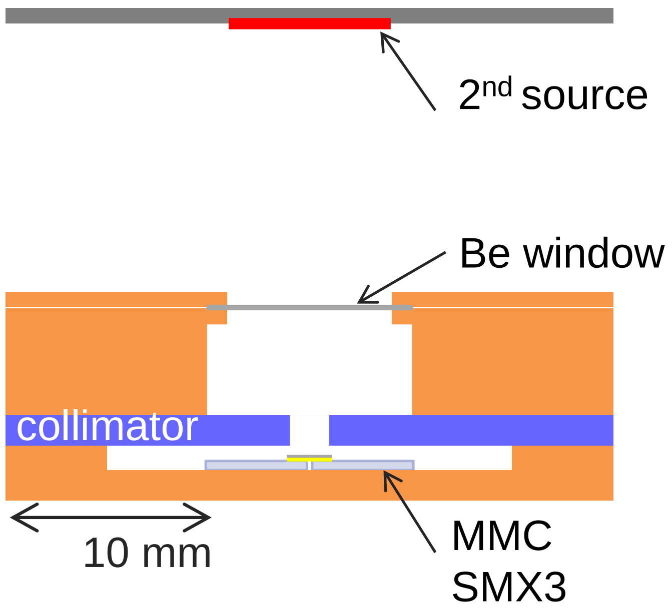

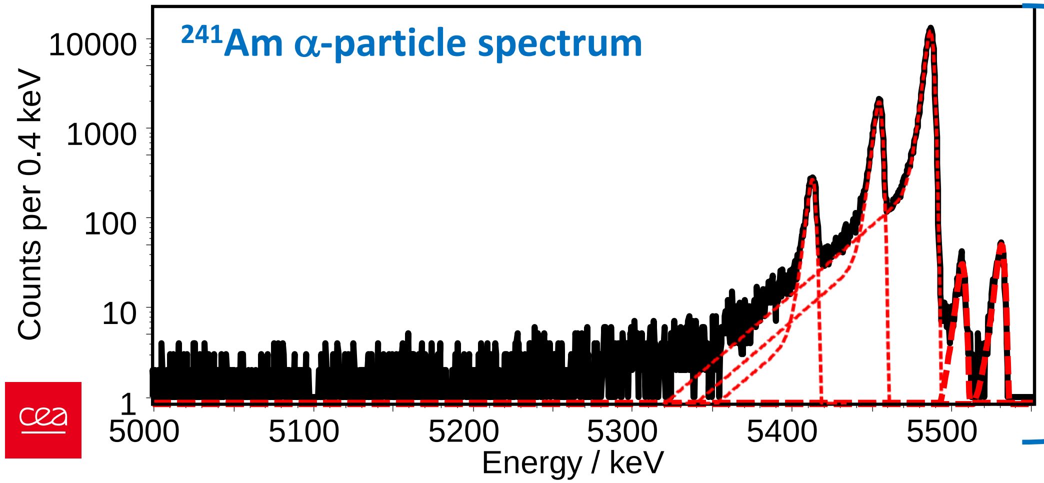

$\rightarrow n_\alpha$

$n_{FEP} \leftarrow$

L X-ray spectrum of ^{241}Am(α) → ^{237}Np

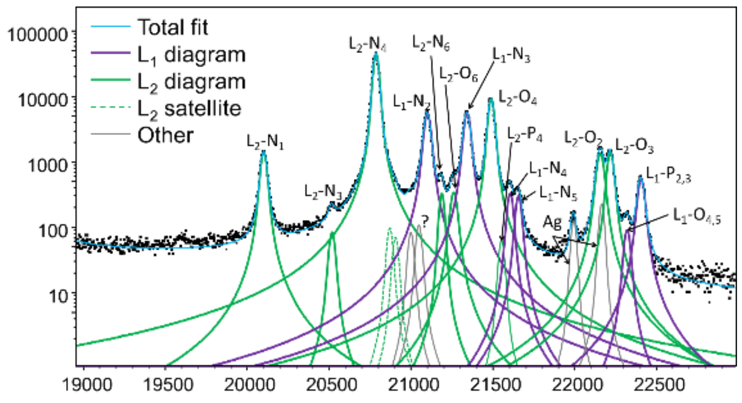

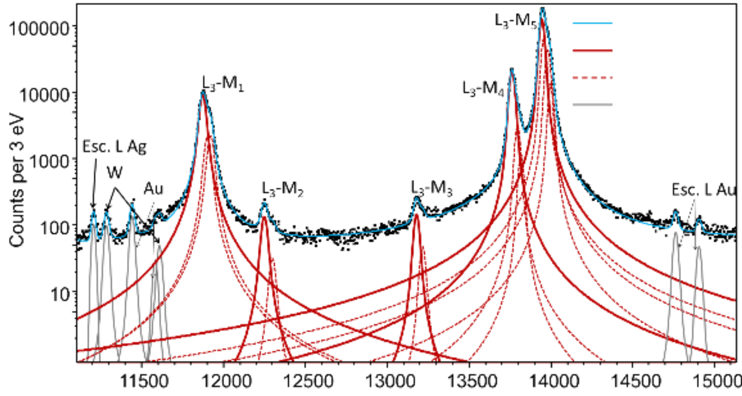

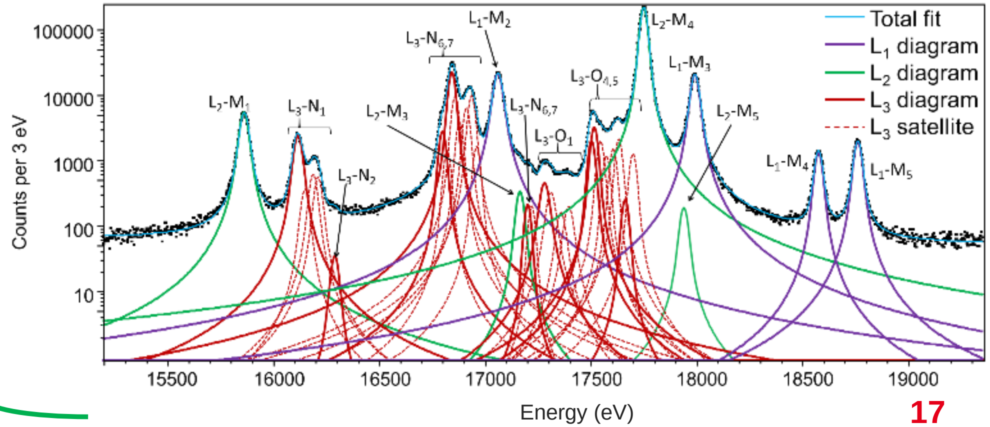

Additional corrections due to the measurement of 2 sources

$$I(E) = \frac{n_{FEP}(E)}{n_\alpha} \frac{F_A \cdot F_{source} \cdot \varepsilon_{int,\alpha}}{\varepsilon_{int,ph}(E) \times t_{Be}(E)}$$

- n_{FEP} and n_α from energy spectra
- F_A ratio between source activities determined by conventional α-particles spectrometry
- F_{source} correction factor for the inhomogeneity of the surface source activitiy determined by radioactive source imager.

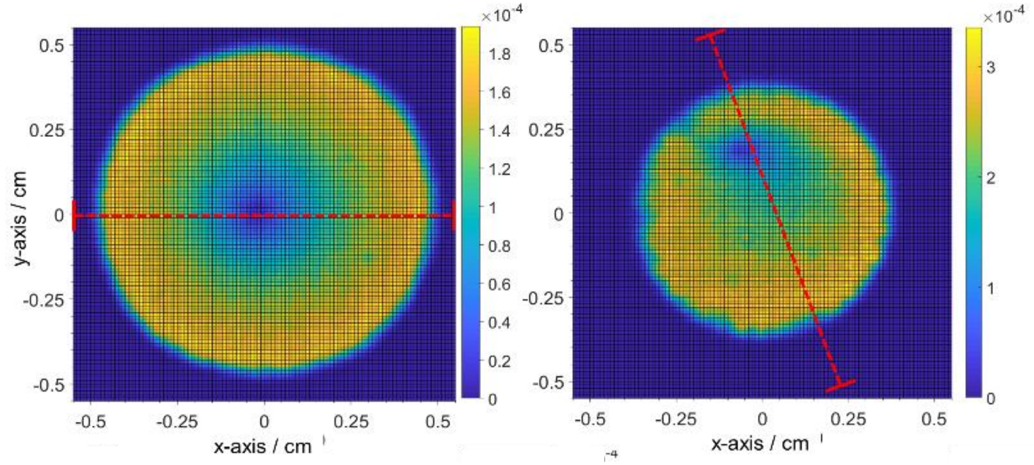

- $\varepsilon_{int,\alpha}$ and $\varepsilon_{int,ph}$ intrinsic efficiencies ~ 1, determined by Monte Carlo simulations.
- t_{Be} transmission through Be window, calculated.

Matias Rodrigues *et al* 2023 *Metrologia* **60** 025005
DOI 10.1088/1681-7575/acb99f

Results of L X-ray PEIs from $^{241}Am(\alpha) \rightarrow {}^{237}Np$

Total L X-ray emission intensity

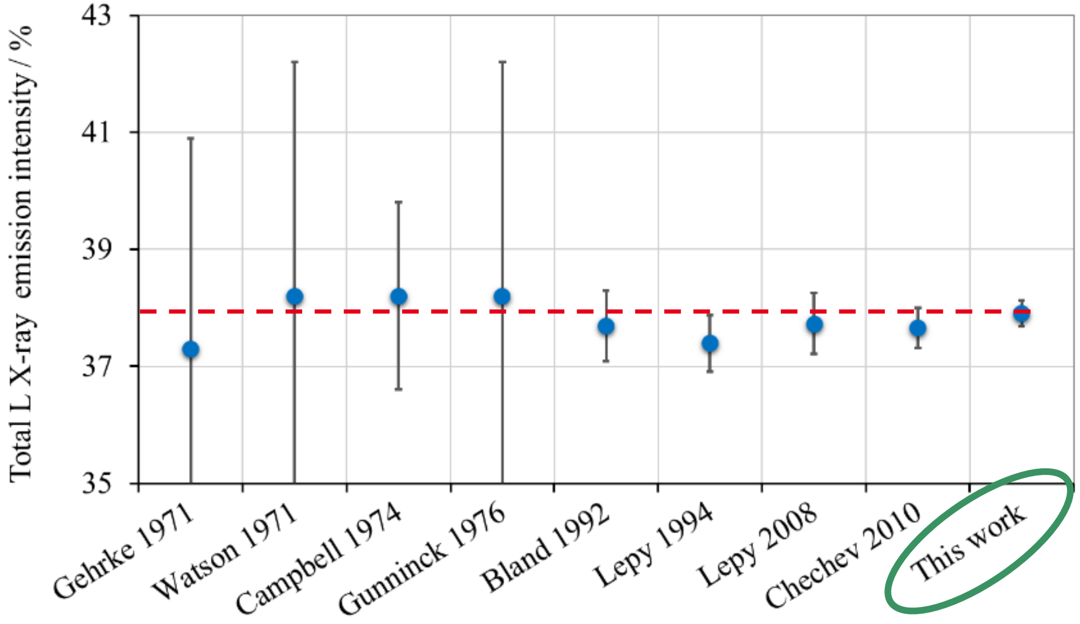

$L\beta\eta$ X-ray emission intensity

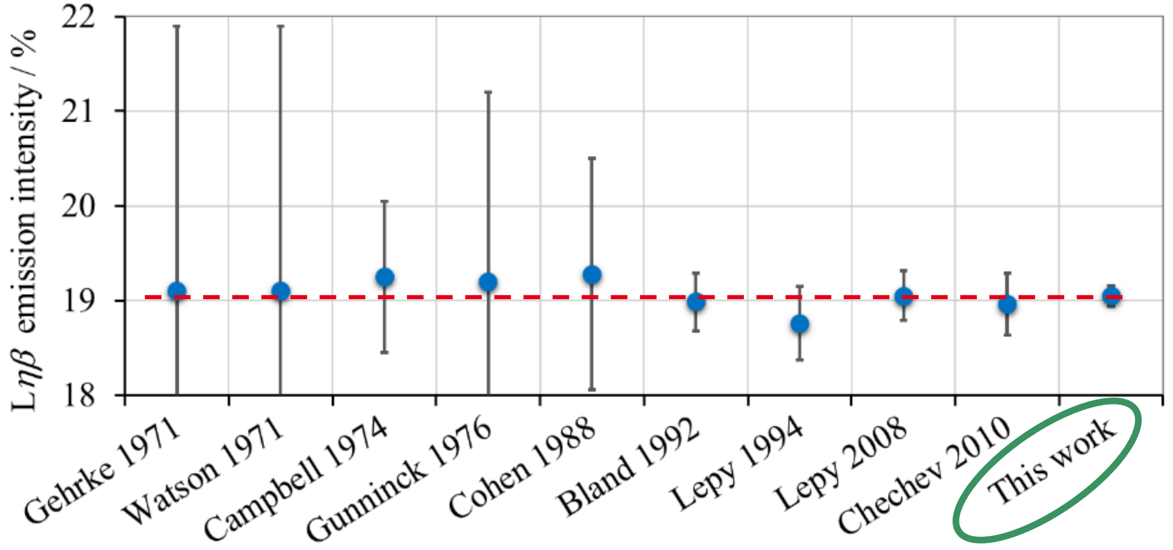

- Good agreement with all the previous published data
- Relative uncertainty (0.32%) 2 times lower than the most precise measurement

Matias Rodrigues *et al* 2023 *Metrologia* **60** 025005
DOI 10.1088/1681-7575/acb99f

Gamma transition energies of ^{229m}Th

^{229m}Th have the lowest gamma transition energy @ 8 eV.
Many possible applications and investigations : nuclear gamma laser, highly accurate, and stable ion nuclear clock to a compact solid-state nuclear clock.

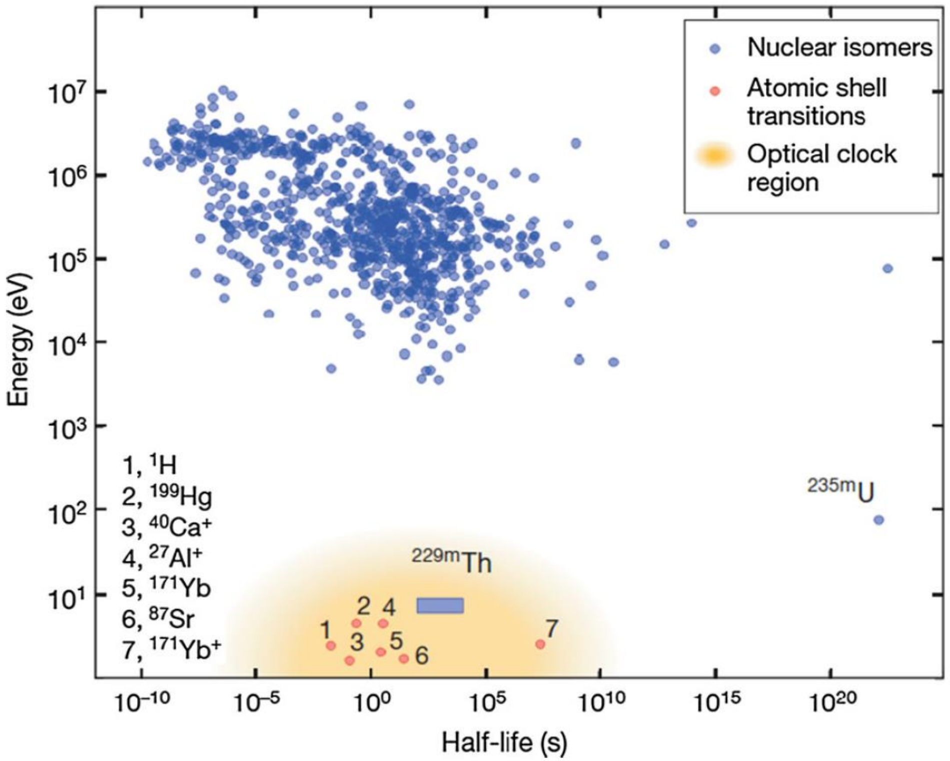

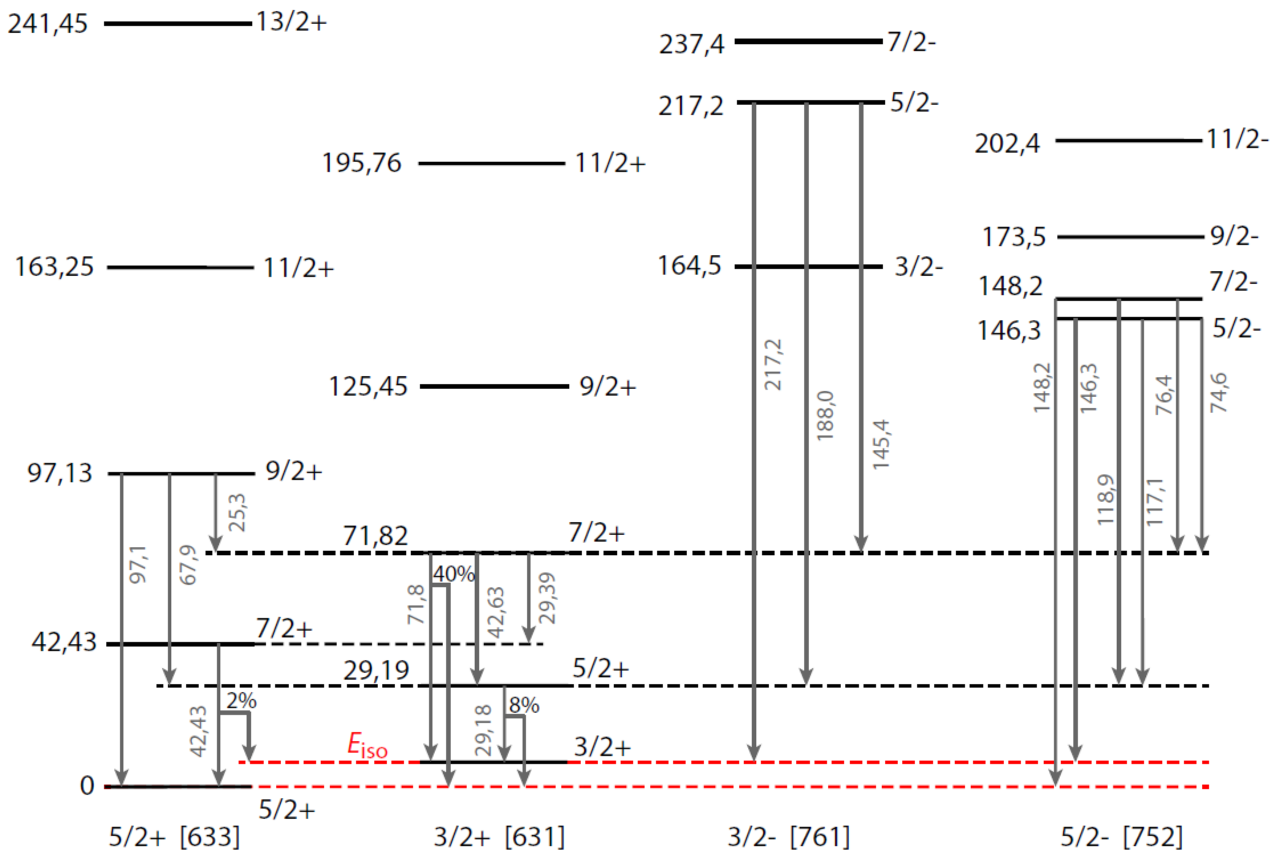

Gamma transition energies of ^{229m}Th

^{229m}Th have the lowest gamma transition energy @ 8 eV.
Many possible applications and investigations : nuclear gamma laser, highly accurate, and stable ion nuclear clock to a compact solid-state nuclear clock.

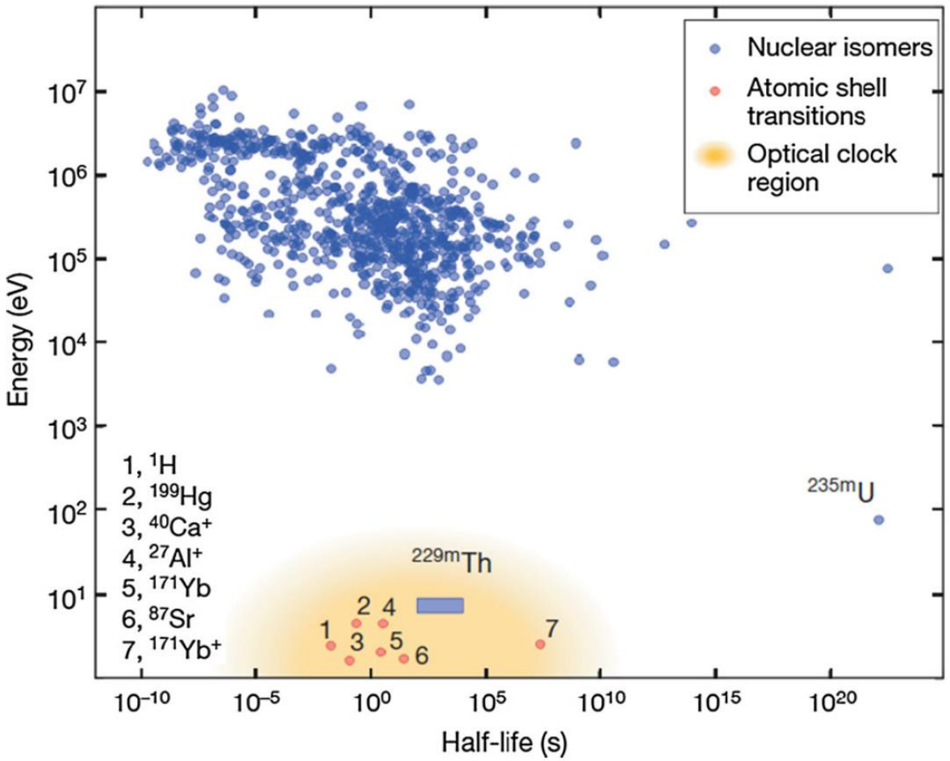

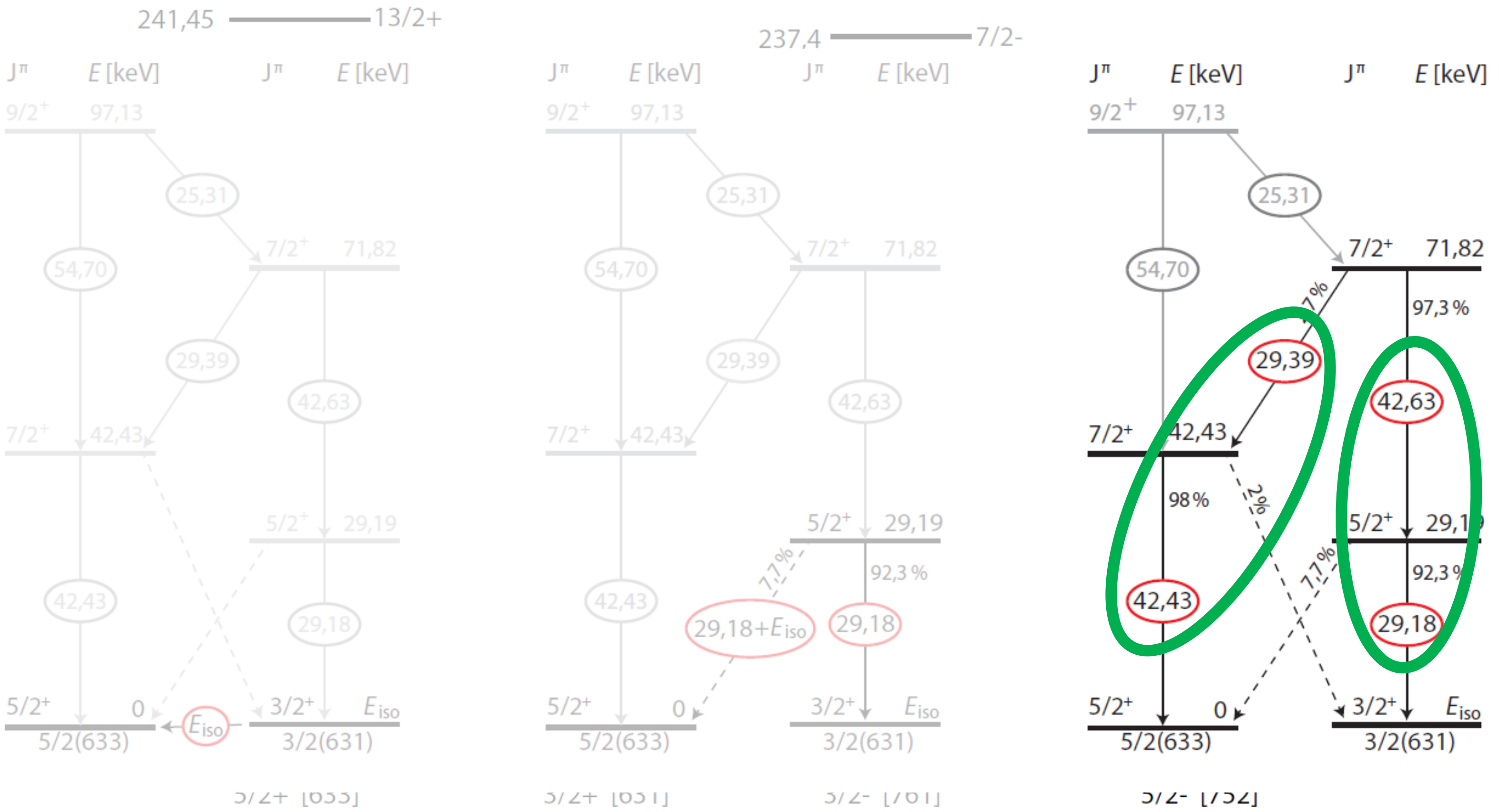

MMC for gamma-spectrometry of ^{229m}Th

- 64 pixel of Au absorber 20x500x500x μm^3
- 32 2-stage DC SQUID read-out
- External source of $^{233}U \rightarrow {}^{229}Th + \alpha$

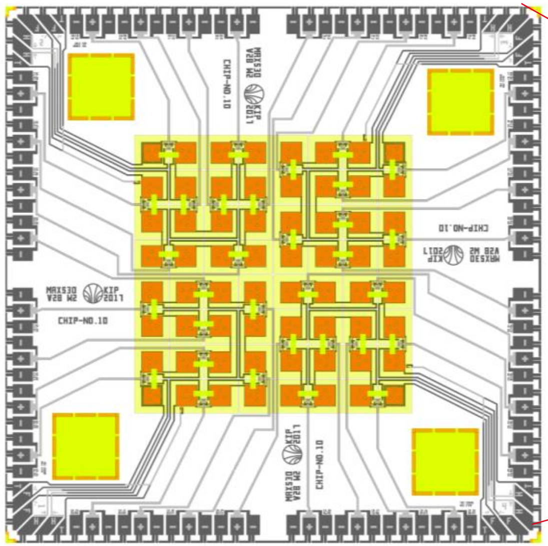

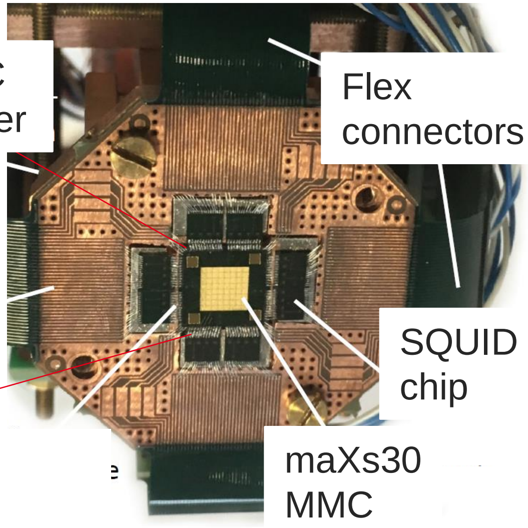

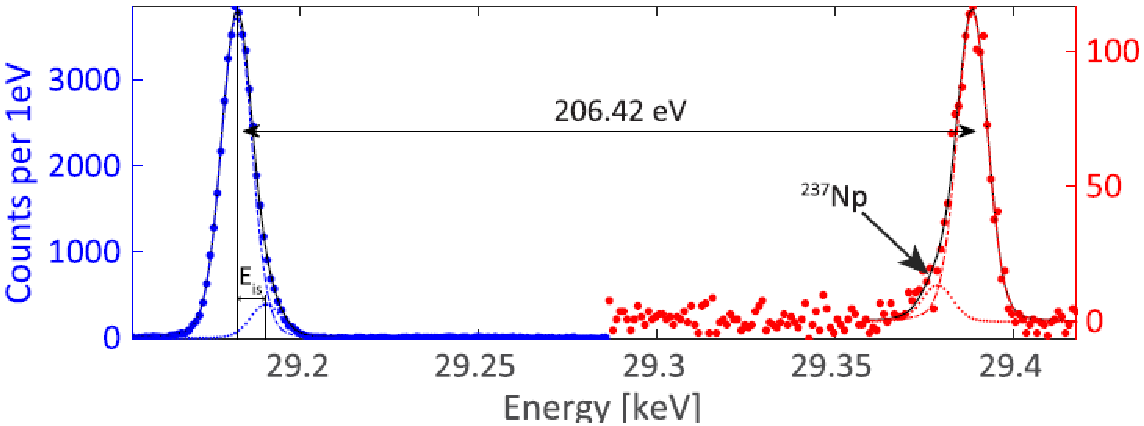

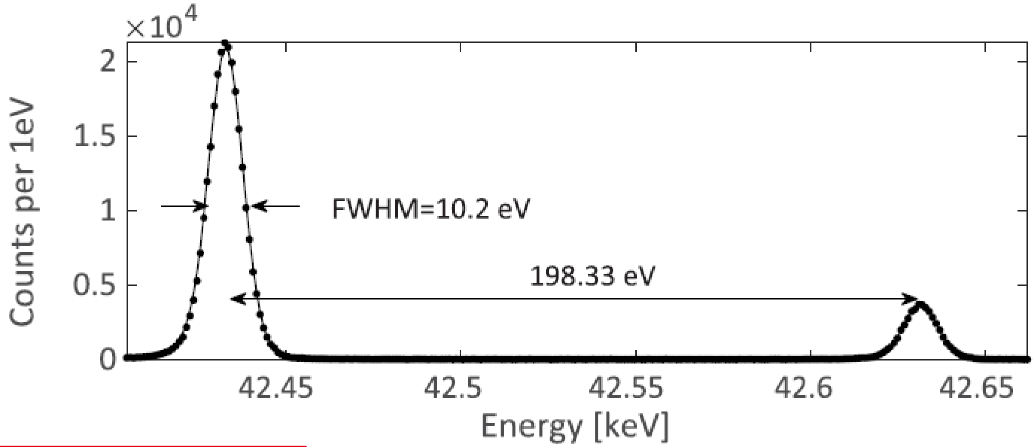

$E_{\gamma,iso}$ = 8.10(17) eV

"Bestimmung der Isomerenergie von 229Th mit dem hochauflösenden Mikrokalorimeter-Array maXs30", Dissertation, Heidelberg 2020
Sikorsky Tet al. 2020 Measurement of the Th 229 Isomer Energy with a Magnetic Microcalorimeter *Phys. Rev. Lett.* **125** 142503

Energy calibration of the MMC

MMC non-linearity

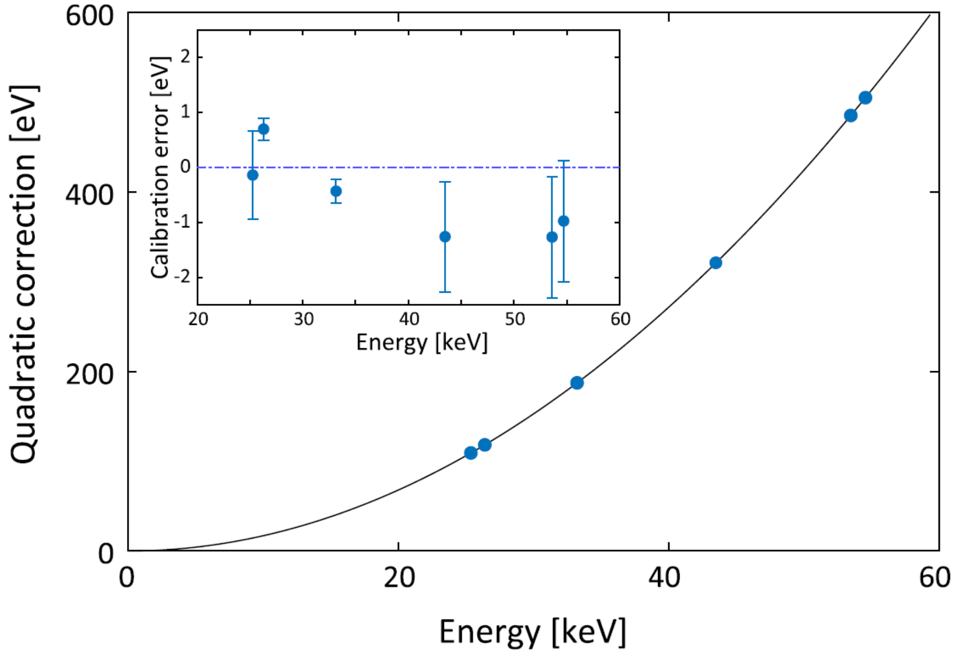

MMC non-lineary calibraction with γ-ray lines

ADC non-linearity

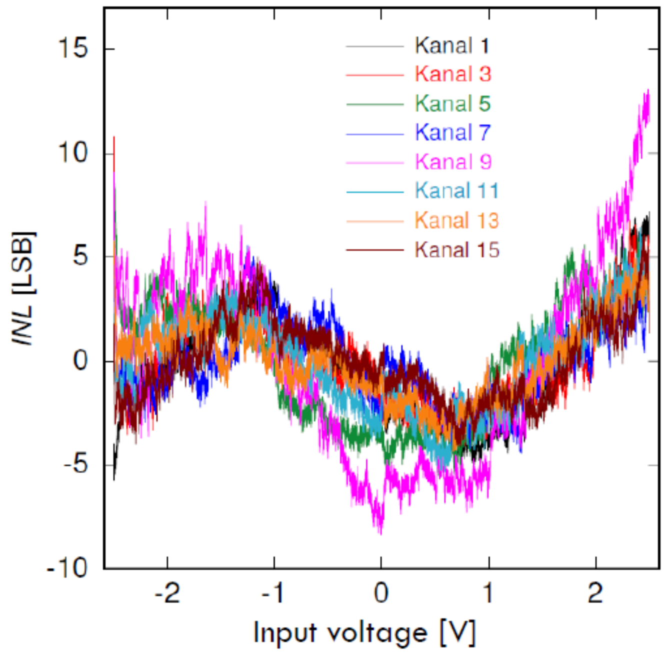

Pulse height deviation due to the ADC

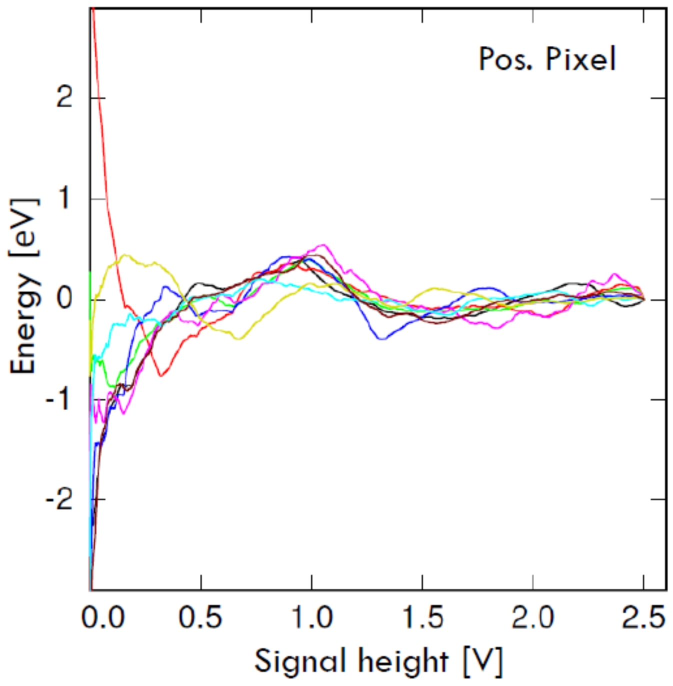

"Bestimmung der Isomerenergie von 229Th mit dem hochauflösenden Mikrokalorimeter-Array maXs30", Dissertation, Heidelberg 2020

Sikorsky Tet al. 2020 Measurement of the Th 229 Isomer Energy with a Magnetic Microcalorimeter *Phys. Rev. Lett.* **125** 142503

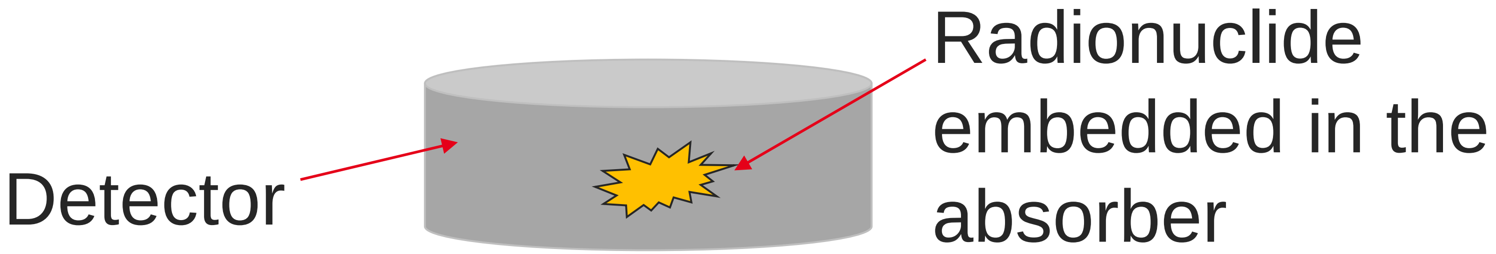

2. Decay energy spectrometry

Activity measurement by DES of β decays

- Beta minus (β⁻) decay $^{A}_{Z}X \rightarrow {}^{A}_{Z+1}Y + \beta^{-} + \bar{\nu}_e$

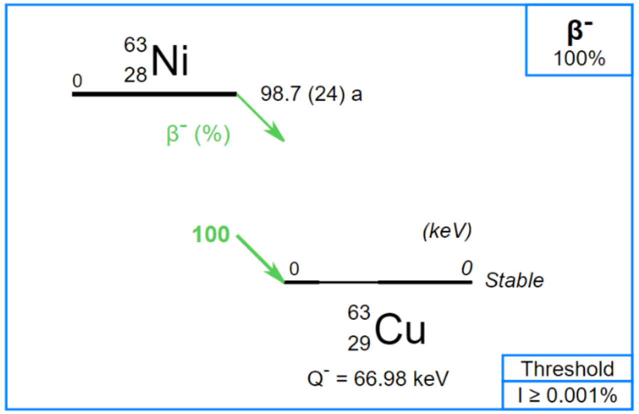

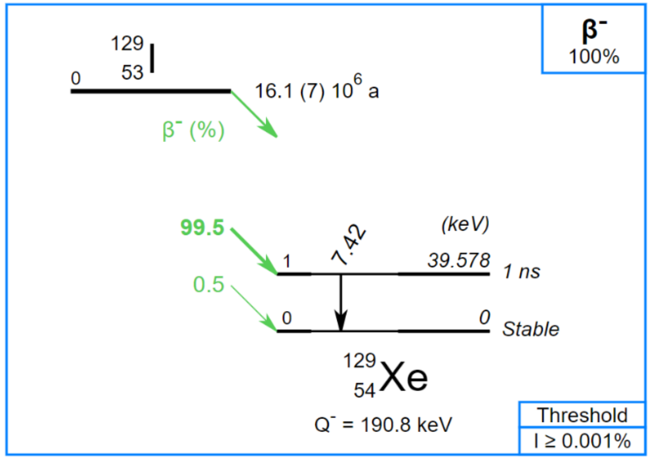

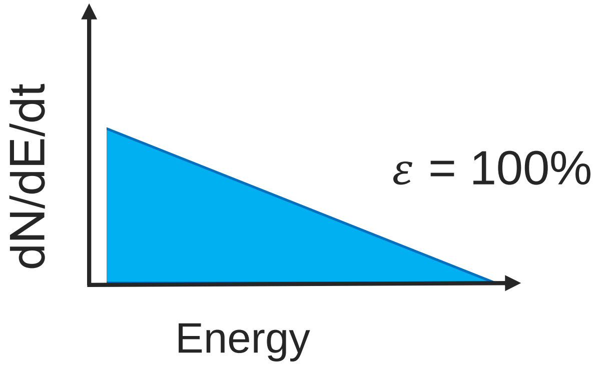

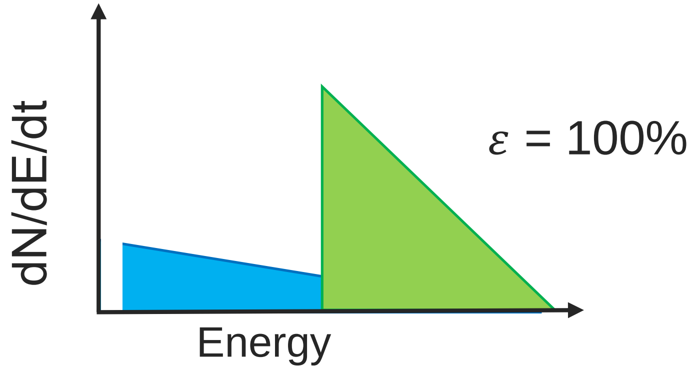

- One beta spectrum
- Two beta spectra

Spectrum area = activity

Activity measurement by DES of EC decays

- Electron capture decay $^{A}_{Z}X + ^{0}_{-1}e^{-} \rightarrow _{Z-1}^{A}Y + \nu_e$

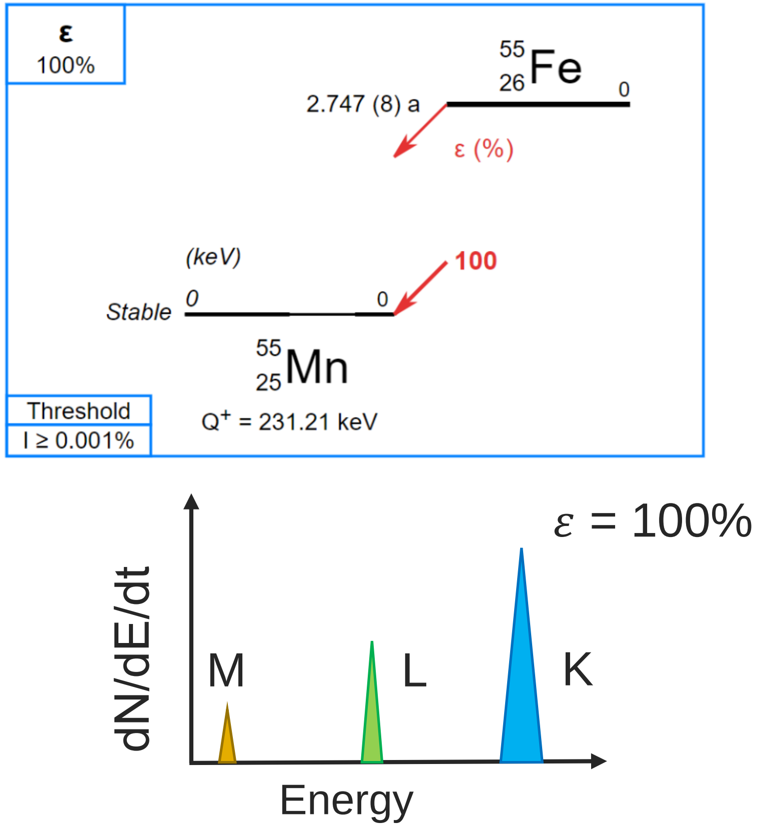

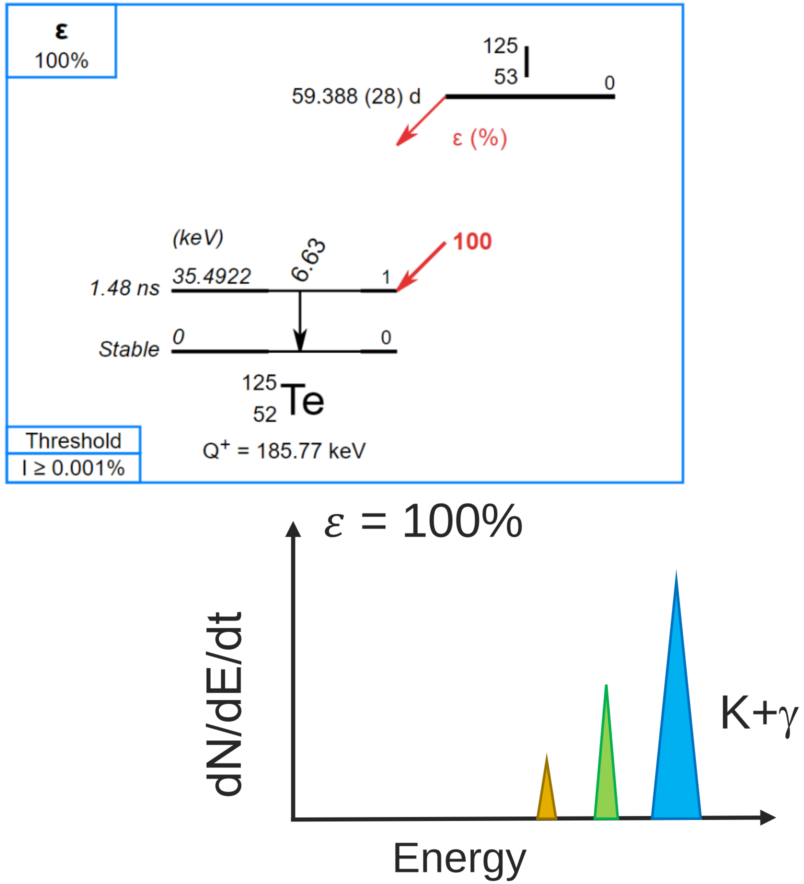

- One peak per electron shell energy of the daughter atom
- Sum of peak areas = Activity
- Individual peak area = electron capture probability

Activity measurement by DES of α-decays

- α-decay $\,^{A}_{Z}X \rightarrow \,^{A-4}_{Z-2}Y + \,^{4}_{2}He$

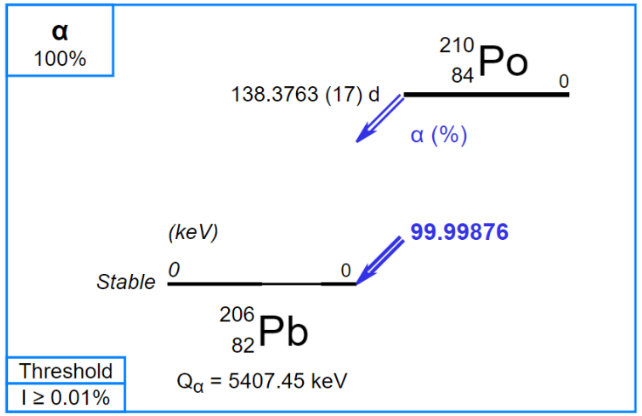

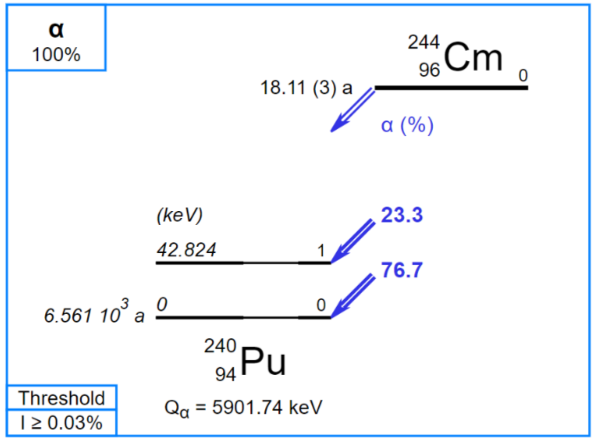

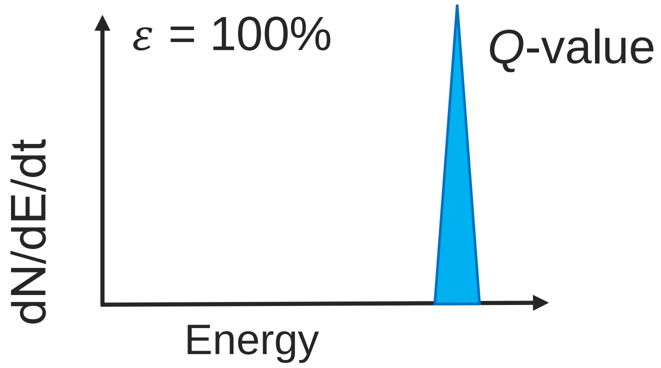

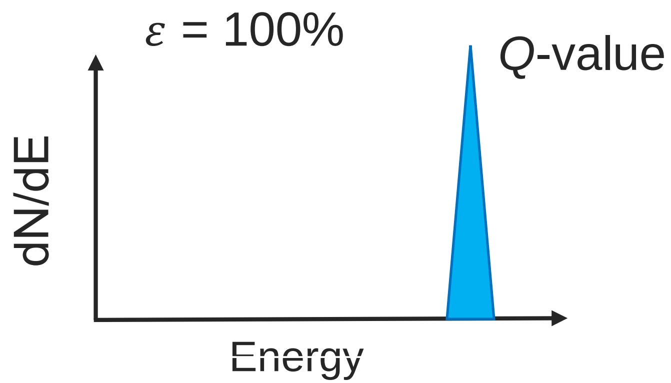

- Peak area = activity
- One peak at ~ the Q-value, characteristic energy for each alpha emitter

→ ideal for isotopic analysis

Activity measurement

Radioactive solution to standardize

Source fabrication

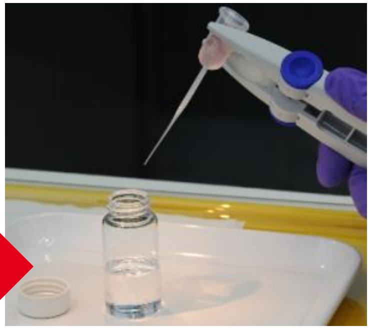

Deposition of solution using a pycnometer

Weighting of pycnometer for traceability of the deposited mass (~ 10 mg)

g

Sources

Activity measurement of the sources by primary methods

- LSC counting (CIEMAT/NIST – TDCR)
- Coincidences
- Proportional counters
- Well-type detector

$$A = \frac{N}{\Delta t \cdot \varepsilon}$$

Bq

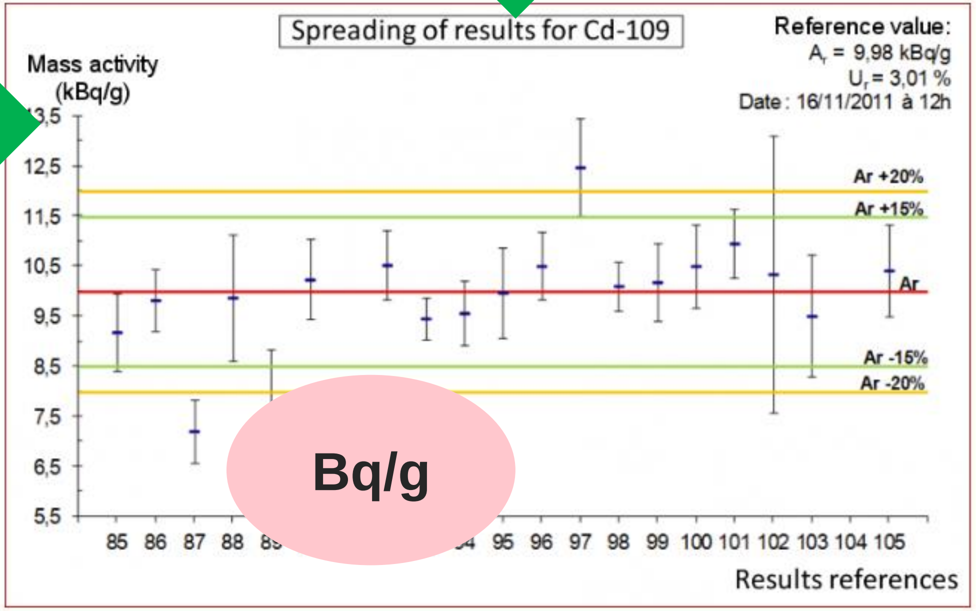

Bq/g

Activity standardization with LSC

- Liquid Scintillation Counting (LSC) is the main method for activity standardization of
  - Pure beta emitters: i.e. C-14, Tc-99, Ni-63
  - Pure Electron Capture: Fe-55, Ni-59…

- Counting efficiency in LSC methods depend on the electron energy spectrum:
  - CIEMAST/NIST methods $$\varepsilon = \int_0^{E_{max}} S(E)(1-e^{-\eta})^2 dE$$
  - TDCR methods $$TDCR = \frac{R_T}{R_D} = \frac{\int_0^{E_{max}} S(E)(1-e^{-\eta})^3 dE}{\int_0^{E_{max}} S(E)(3(1-e^{-\eta})^2 - 2(1-e^{-\eta})^3)dE}$$

Birks's expression

$$\eta = \frac{v}{n}\int_0^E \frac{A\,dE}{1 + kB\frac{dE}{dx}}$$

Problem: light emission, is a non-linear function of electron energy E.

→ LSC activity measurements depends on the decay scheme and on fundamental parameters

→ DES with LTDs can be a alternative method for these radionuclides

Comparison of the measurement from MMCs with other established methods

Established methods:

- Activity for sources with **activities > 100 Bq.**
- Solid sources prepared from **~ a few tens of µL**
- Source an area of about 1 cm^2.

Problem

1 order of magnitude

LTDs

- Typical count rate capability per absorber of **a few s^{-1}**
- Typical absorber has area below a few mm^2

Deposition of ~100 Bq on 1 cm^2

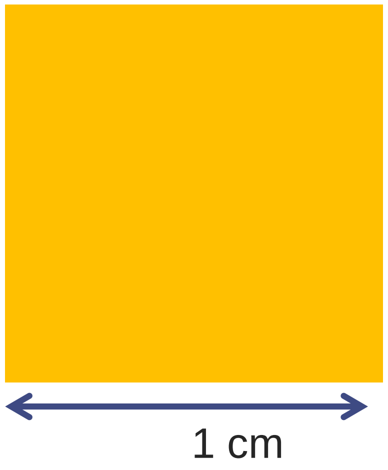

Solution

Separation into 25 sources

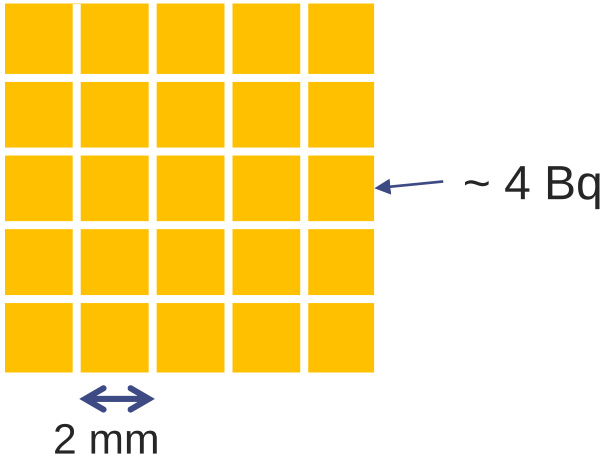

→ Secondary sources embedded in 4π absorbers
→ activity measured by multi-channel MMCs

Characterisation of the source ^{241}Am with the copper mask

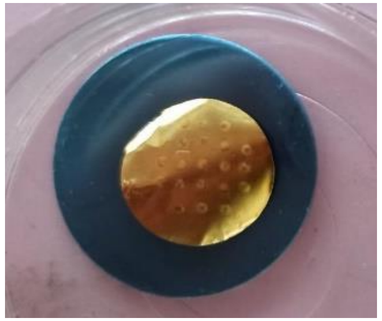

~ 21 available circular sources

- Deposits hardly visible
  - □ better α-spectrum resolution
- A = 16.64 Bq
  - □Lower deposited activity because the cooper mask is also deposited

Alpha spectrum with a semiconductor

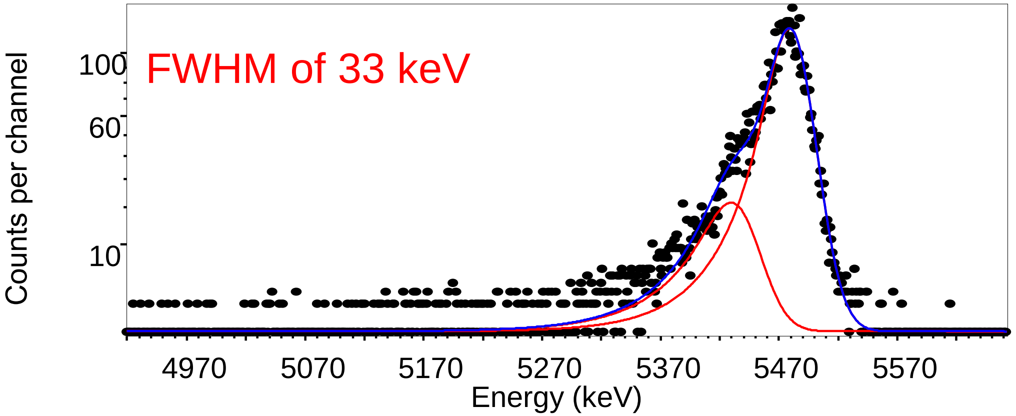

Autoradiography

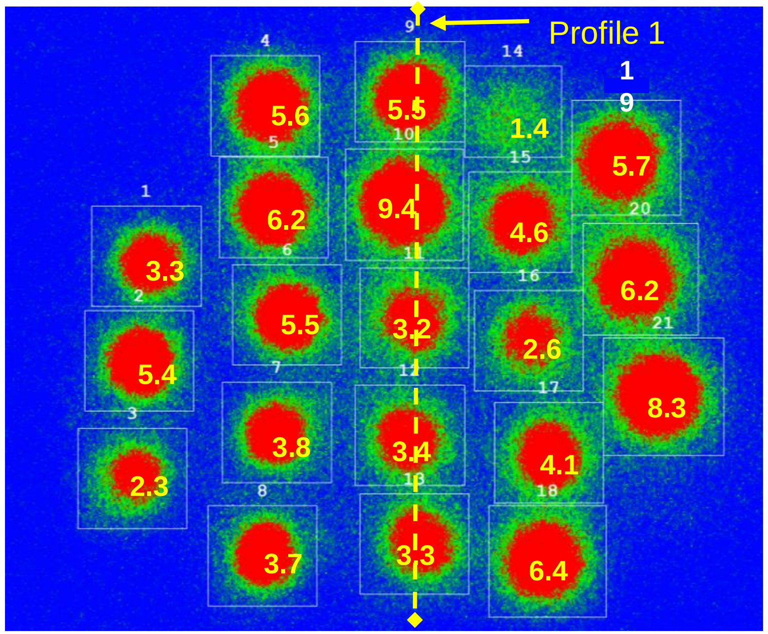

Profile 1: through the circles

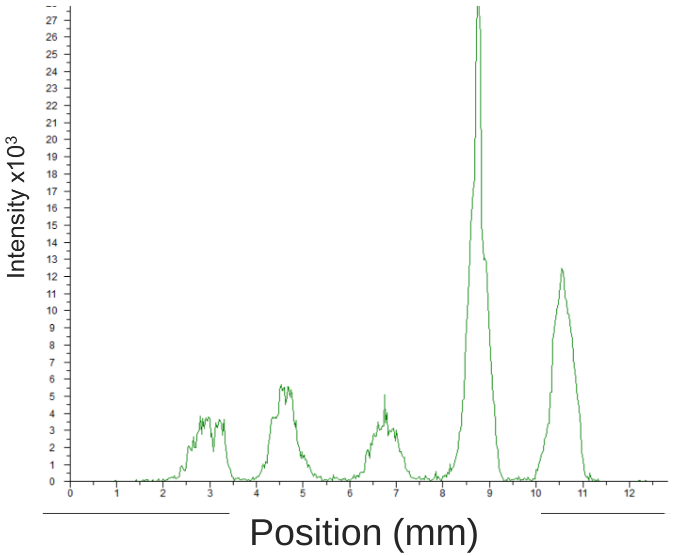

Multichannel set-up for 10 MMCs

PrimA-LTD

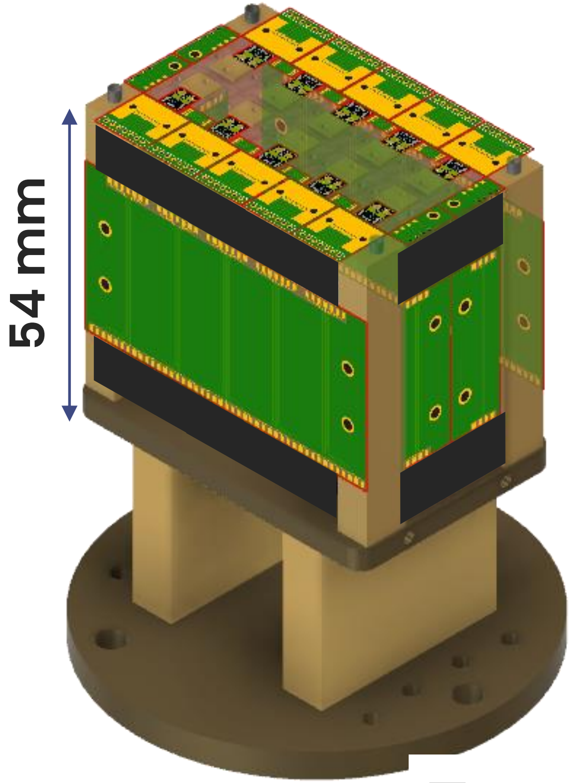

Base plate connected to mixing chamber

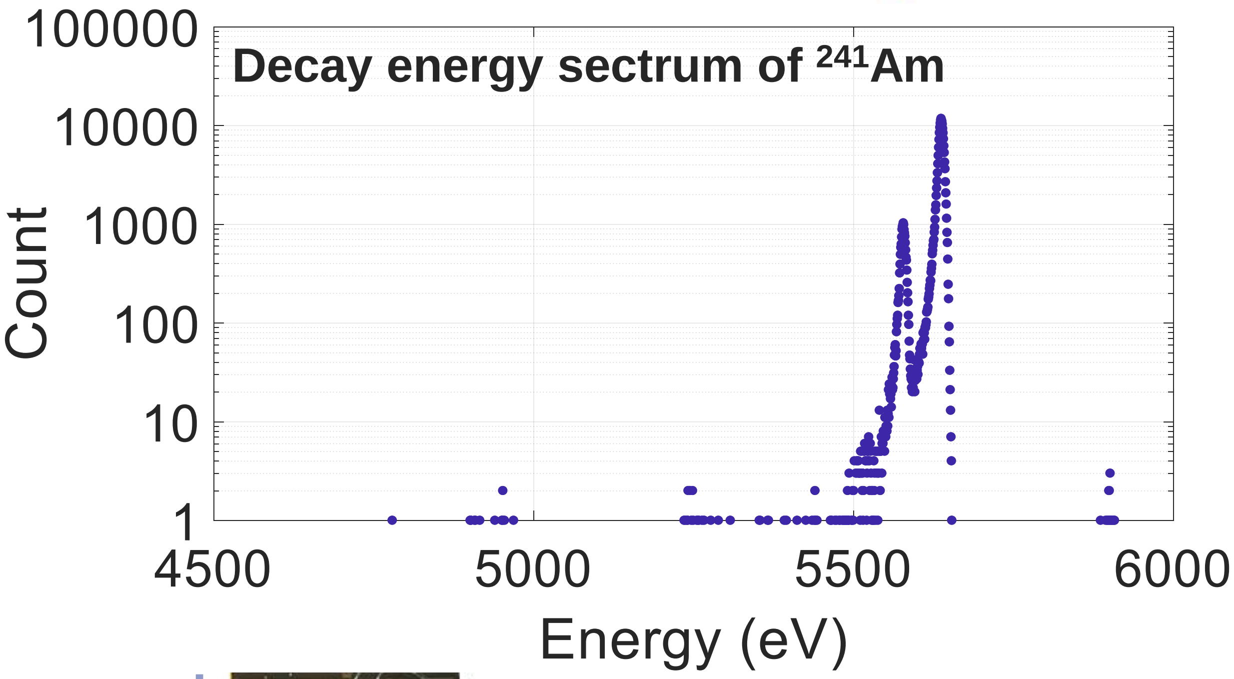

Top view

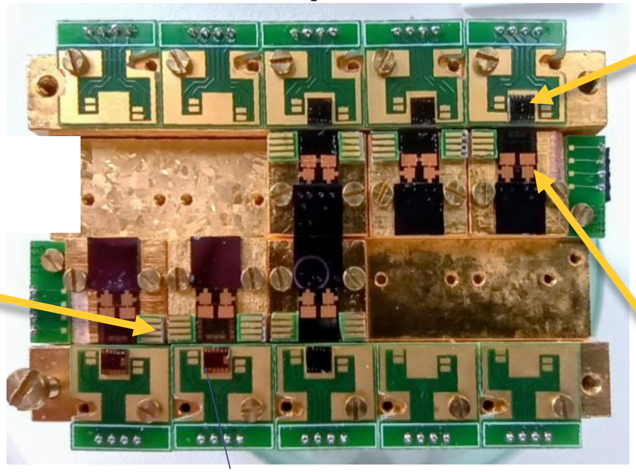

SQUID

PCB for daisy-chaining

ROS-L MMC

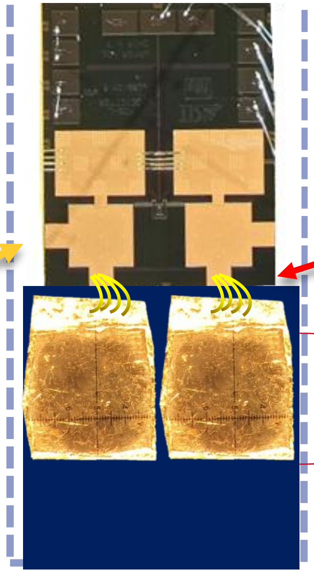

Si plate for absorber

25 µm thick Au strip

25 µm diameter bonding wires

200 µm thick absorber

Comparison of the activity measurement of the ^{241}Am source between different labs

PrimA-LTD

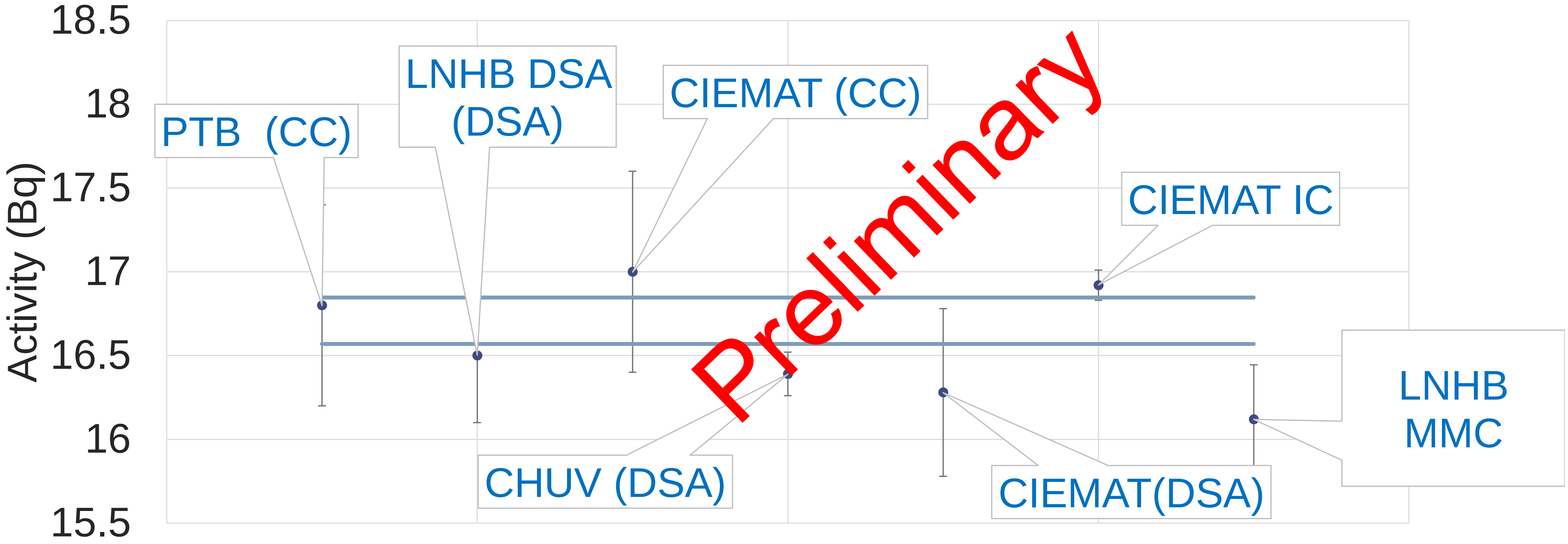

CC = coincidence counting
DSA = Defined Solid Angle
MMC = Metallic Magnetic Calorimeter
IC = Ionization chamber

Beta spectrum of ^{151}Sm branch probabilities and end-point

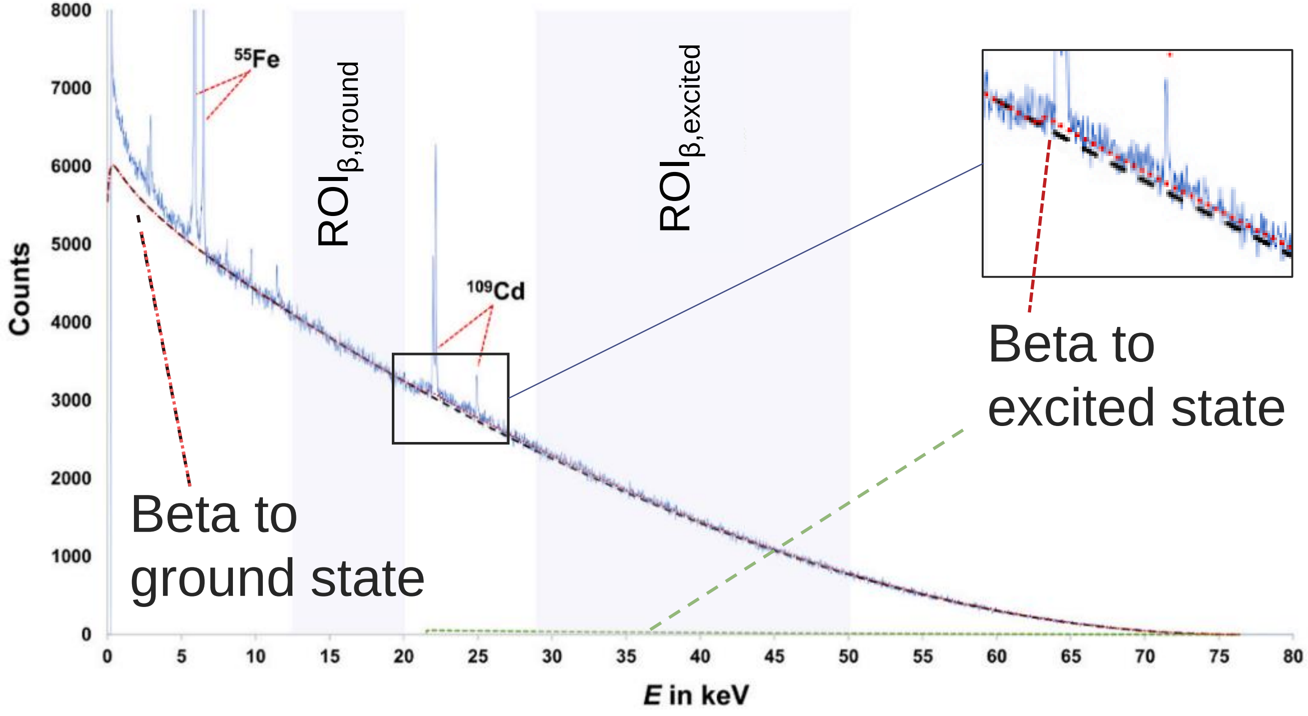

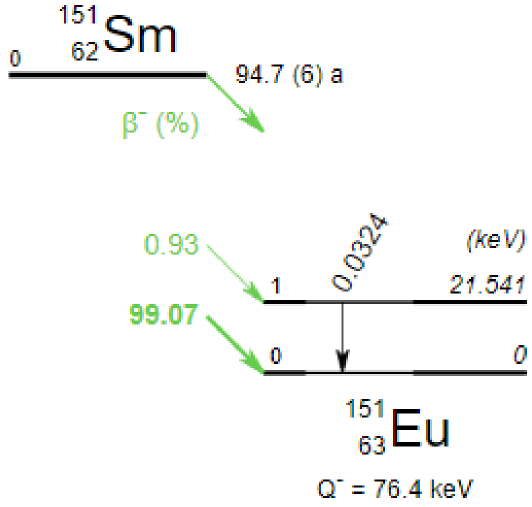

- Measured $P_{\beta,ground}$ = **99.31 (11)%** and $P_{\beta,excited}$ = **0.69 (11)%**

  Recommended value DDEP: **99.07 (4)%** and **0.93 (4)%**

- Measured E_{max} = **76.430 (68) keV.**

  Recommended value AME2020: **76.5 (5) keV**

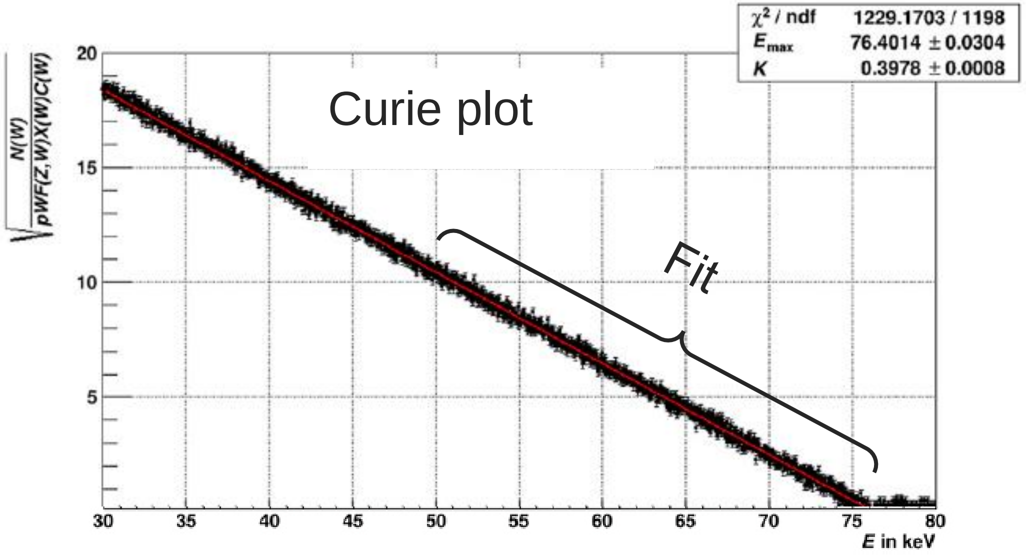

K. Kossert, ARI, Vol. 185, 110237, 2022
https://doi.org/10.1016/j.apradiso.2022.110237

Applications using quantitative analysis by DES with LTDs

- Activity measurement ongoing development
  - Fe-55 @ PTB
  - Am-241 @ LNHB
  - Am-241 @ NIST

- Decay data
  - End-point energy of beta spectra
  - Beta shape
  - Electron capture probabilities

- Safeguards
  - isotopic analysis of Pu

- Impurity measurement
  - Radiopharmaceuticals (Ac-227/Ac-225)

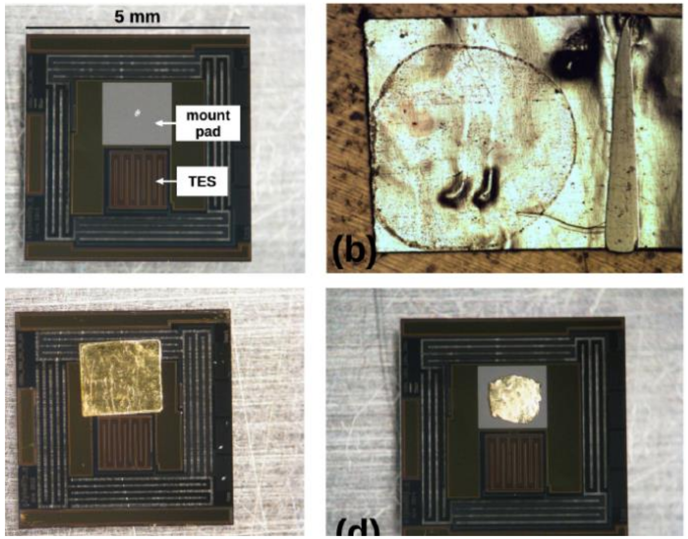

Hoover A.S., 2015, Anal. Chem. 2015, 87, 3996−4000

Merci